SIMULATION STUDY OF THERMAL ELECTRIC CIRCUIT

By

Dafa Yan

A THESIS

Submitted to
Michigan State University
in partial fulfillment of the requirements
for the degree of

Mechanical Engineering—Master of Science

2014

ABSTRACT

SIMULATION STUDY OF THERMAL ELECTRIC CIRCUIT

By

Dafa Yan

Thermoelectric generator works under different working conditions, especially different temperature and load resistance. In order to improve its efficiency, the circuit was in place between thermoelectric generator and load resistance using a buck converter. Compared with the direct connection case the buck converter improves efficiency, especially with small load resistance. Power output and current ripple are the central focus for evaluating this buck converter.

Regarding thermoelectric generator characteristic, PMW (pulse-width-modulation) mode is selected for regulating buck converter switch. The tool box selected for building simulation model of buck converter is Simscape in matlab/Simulink. To verify the model, differential equation mathematic model and state-space simulation model are built. To configure the parameters of the buck converter, all the possible data is collected by running simulation model with different sets of parameters. After configuration, the optimal parameters for the buck converter is obtained. A method of selecting optimal parameter set is introduced for the given requirement for the circuit performance.

With a set of optimal circuit parameters such as capacitor and inductor values, a controller of PWM signal is to be designed for optimizing the circuit system efficiency, where the extreme seeking control was used. With the controller, it proves that even with different load resistance, the buck converter can delivered maximum power with optimized the duty cycle of PWM.

ACKNOWLEDGEMENTS

It has been two years since I enrolled in Michigan State University. Every slightly progress I made here comes from continual support from my professors and friends. I would like to first and foremost thank my academic advisor, Professor George Zhu. Even before we met each other, he had already began to inspire me for a perspective future through email communication. I would never forget the moment that he welcomed me in his office for my first time at MSU. I was so worried and confused about my future as a new student at that time. His kindness and patience filled me full of hope and confidence. With his encouragement and direction at the beginning of my harsh life in MSU, I overcame many difficulties and set up my mind to become a control engineer. During the academic life at school, he is always nice and cared about me. He pushed me when I was lazy and encouraged me when I got depressed. He helped me plan my future and taught me how to communicate and behave as a good engineer. I always feel full of courage and confidence with his standing behind me. I know this is not only for now, but forever. What I learned from him is not only the knowledge about engineering but also the truth in life. I will thank him forever.

I would like to thank my committee members, professor Choi and professor Schock. I always recalled the direction from professor Choi in nonlinear control course. Every time I stepped into his office seeking for help about the course project, he always directed me patiently and answered my question. I would like to thank professor Schock for his kindness to let me sit in his engine class. The engine knowledge I learned in his lecture is truly necessary in my career.

I would like to thank my friends in our lab. I have to say that my life is enriched and much better because of them. Yingxu Wang is the first friend I made in Michigan State University. He is always the first one who comes to my mind when I need help. Jie Yang is always avid to help me and support me as a reliable senior. Shupeng Zhang taught me control knowledge continually. With his help, I started to find that I have enthusiasm of learning control. I will never forget the studying time I spent with Yifan Men. We were partners of conducting this research at the beginning. The research life we shared together was happy and harvest. Tao Zeng treated me as one of his best friends. He is always willing to share my problems both in life and study selflessly. Ruitao Song is the one I truly appreciate for this thesis. He really helped me a lot on state-space modeling and extreme seeking control. Without his help, I could never have my thesis completed well.

After all, I would like to thank my parents. Their supporting is my foundation of finishing master education in America. Everything they did for me and sacrificed for me is unforgettable. I will memorized their cultivation and supporting forever and ever.

TABLE OF CONTENTS

LIST OF TABLES

LIST OF FIGURES

KEY TO SYMBOLS AND ABBREVIATIONS

Ω	Ohm
μF	Microfarad
μH	Microhenry
Am	Ampere
C	Capacitor
CCM	Continuous conduction mode
DCM	Discontinuous conduction mode
F	Farad
H	Henry
Hz	Hertz
I	Current
kHz	Kilohertz
L	Inductor
LQR	Linear-Quadratic Regulator
PFM	Pulse frequency modulation
PWM	Pulse width modulation

PW	Power
PID	Proportional-integral-derivative
R	Resistance
S	Second
t	Time
T	Period
TEG	Thermoelectric generator
U	Direct current electric source
V	Voltage

Chapter 1 Introduction

The thermal efficiency range of gasoline engines are between 25% and 40%. Half of the rejected heat is carried away by the exhaust gas emission. Reusing the exhausted energy is a very important as improving energy efficiency is urgent due to limited energy resource. A significant role is played by thermoelectric generator that utilizes the waste exhaust energy. Load and internal resistance of a thermoelectric generator circuit changes continuously as the exhaust gas temperature varying. In order to maximize the power output of a thermoelectric generator, optimization of thermoelectric generator circuit with on-line control is necessary.

1.1 Thermoelectric Generator Overview

To convert thermal energy into electricity, 100 watt skutterudite thermoelectric generator designed and developed by MSU was applied as the foundation for studying thermoelectric circuit in this research. In this skutterudite thermoelectric generator, two materials named N-type material and P-type material are utilized. The characteristic of N-type material drives current toward the hot side whereas the P-type material works in the opposite way. Electromotive force is generated while a pair of N-type and P-type components are exposed to two sides with a temperature gradient. An Electricity source is formed while several of these power units connect in series. The advantages of thermoelectric generator is highlighted on its quiet working property and widely used in some special cases. The thermoelectric generator can be applied in exhaust system of vehicles such as exhaust pipe, EGR (exhaust gas recirculation) cooler, and even on engine wall [1].

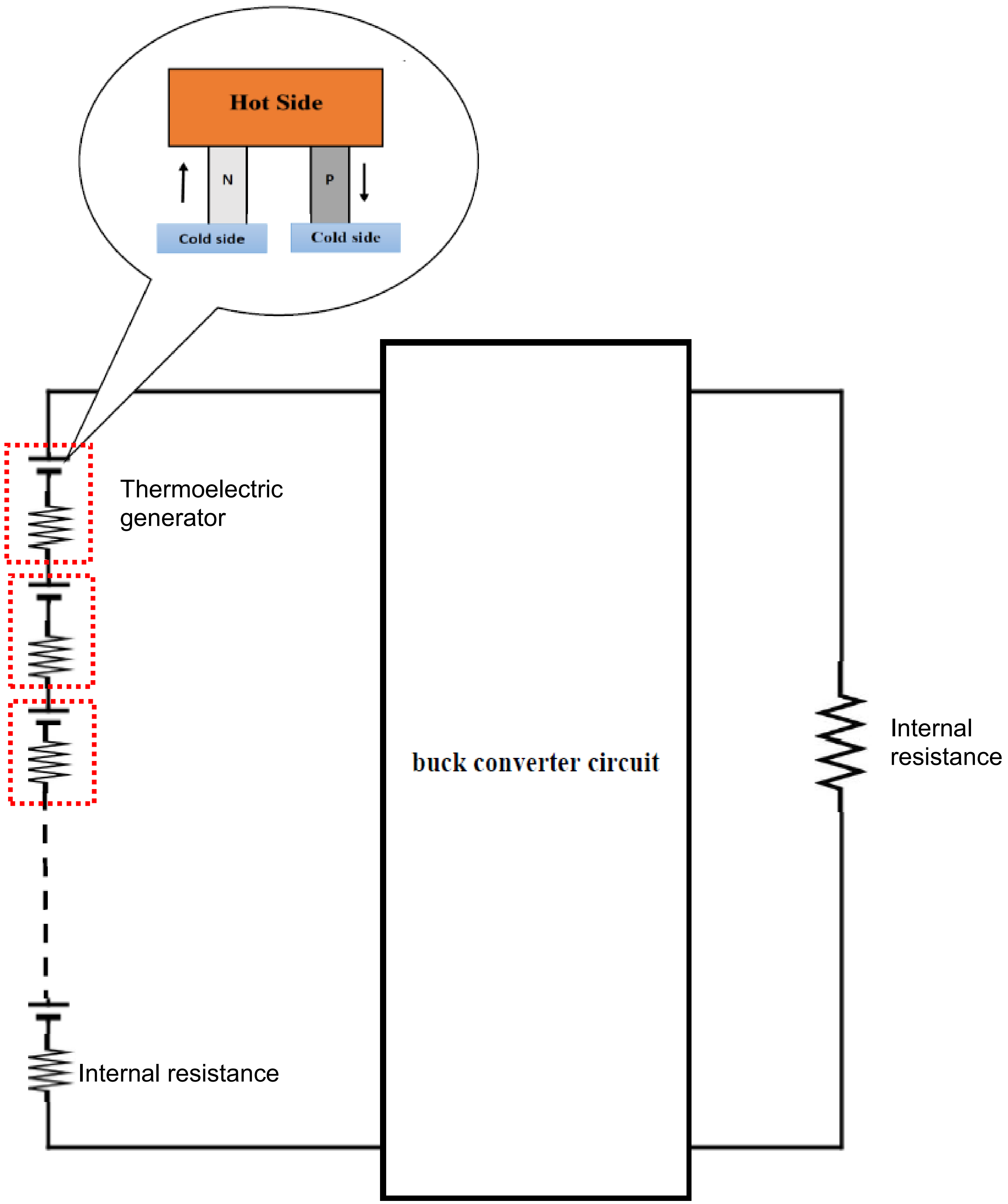

Figure 1-1 Thermoelectric generator

1.1.1 History of Thermoelectric Generator

Thermoelectric generator is a widely-used electric generator due to its advantages mentioned before. The theoretic foundation of thermoelectric generator was formed as a discovering in 1821 AD by Thomas Johann. As there was temperature gradient over the compass which was made by two different metal materials, there was tiny current going through the compass. The deflection of compass caused by electromagnetism was the proof that there was current generated by the temperature gradient over two type metals when they were connected.

In 1834 AD, the phenomenon that heat would be generated at the junction of two types of metals while a current was amounted over it was discovered by a French physicist Jean Charles Athanase Peltier. By reversing the current, the cooling effect would also be detected. The relationship between current and the heat absorbed or generated by the current is proportional.

William Thomson was the one who made the conclusion and the connection of these two theories based on thermodynamic theory. The theory, named as Thomson effect, states that the heat absorbed or created by thermocouple is proportional to both current and temperature gradient over the thermocouple.

After the theory foundation has been set, numerous experiments had been done in order to study thermoelectric generator. Three classical applications were introduced as they showed the advantages of using a thermoelectric generator comparing with other electric generators [2].

1.1.2 Application of Thermoelectric Generators in Modern World

Regarding the material and working principle of thermoelectric generators, the benefits of using them is obvious. Especially considering the wide range of application and outstanding efficiency, a commensurate emphasis is given to thermoelectric generator in science research and commercial utilization. Furthermore, the reversibility of thermoelectric couple is also a prominent characteristic which will also have a great effect when it is applied for absorbing heat.

A well-known application example of thermoelectric generator is the Multi-Mission Radioisotope thermoelectric generator designed by NASA for operating on Mars and vacuum of space. Long-lived, reliable and stable power source are needed in space exploration missions as two hazards, radiations and vacuum are concluded by the working conditions of the outer space. These requirements are met successfully by this newly designed power source device, Multi-Mission Radioisotope thermoelectric generator. The two components of this thermoelectric generator are plutonium-238 heat source and thermoelectric couple. By converting the heat generated by plutonium's decay into electricity, the thermoelectric generator can support the spacecraft to work in Mars. In its first working year in Mars, this power system have supported the spacecraft to drive on Mars for more than 1.6 kilometers and send back 190 gigabits data. It also fired more than 75000 laser shots [3].

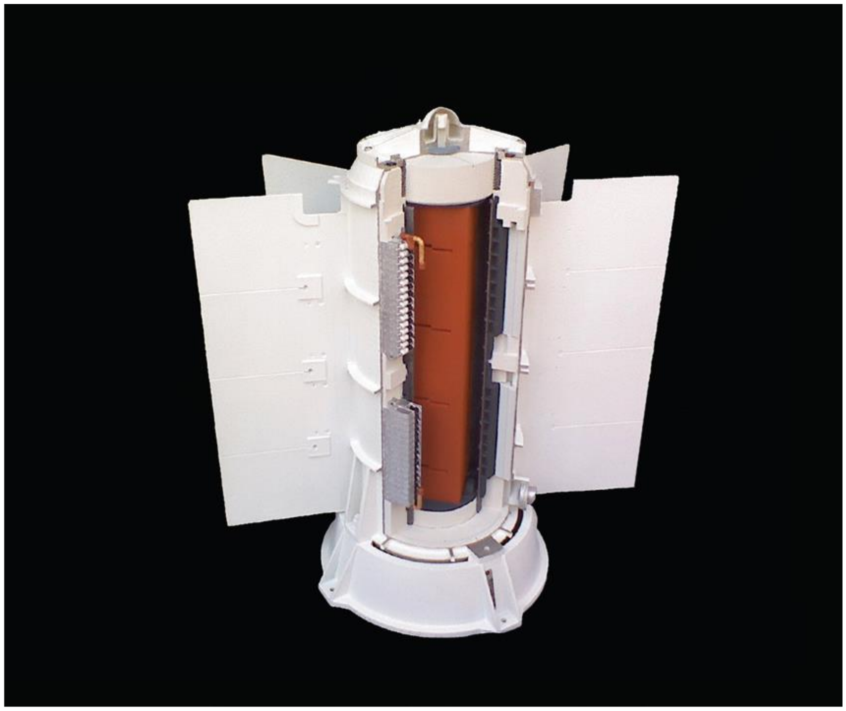

Figure 1-2 Multi-Mission radioisotope thermoelectric generator model

Wearable devices are also a typical application of thermoelectric generator. Google glass is the specific product which can utilize the heat from human body with a thermoelectric generator. Organic material is preferred by human heat thermoelectric generators. The flexibility and compatibility of this kind of material are the crucial reasons for being chosen as the material applied on human skin [4].

This research focuses is placed on the thermoelectric generator which is supposed to be apply in automotive system, especially to the gas exhaust system. Considering the efficiency and economy requirements of automotive industries, thermoelectric generator is unreplaceable. Other than these, the effect on reducing noise and saving space also contributes to the usage of thermoelectric generator. As an example of the benefits from using thermoelectric generator in vehicles, the application in BMW X6 SUVs is persuasive. The thermoelectric generator is designed to be integrated in the radiator of the exhaust gas recirculation system rather than the traditional design method that configures thermoelectric generator as a separate module in the exhaust system underneath vehicle. According the customer testing, fuel consumption is reduced as well as 250 watts electricity was generated by the thermoelectric generator. In the meantime, there is also additional heat supplying to passenger compartment by the thermoelectric generator being configured in this way [5]. Thermoelectric generator is forecasted to play a significant role in energy saving in future.

Figure 1-3 Thermoelectric generator in exhaust gas recirculation system

1.2 Motivation and Strategy of Circuit Optimization

The circuit conducting power generated from thermoelectric couple to load is also a core part of thermoelectric generator. Motivation and strategy of circuit designing are introduced in this chapter. Basic tool for researching the circuit is Matlab/Simulink. The goal circuit is been designed as a buck converter which are used to regulate the load resistor voltage while the value of resistance charges constantly.

1.2.1. Original Circuit Research and Background

Electromotive force can be provided by the circuit source which is connected in series with the thermoelectric couple units. This parameter depends on temperature gradient of circumstance and property of thermoelectric couple. It can be treated as a constant value that cannot be impacted by structure or component parameters of generator circuit. As the working temperature of thermoelectric generator are quite high, the internal resistance of the power source cannot be ignored. An original thermoelectric generator circuit can be simplified as a circuit consisted with one source resistance, one load resistance and a constant voltage source. The load resistance value could vary while the electrical load changes. To demonstrate the original structure well, a circuit is shown in Figure 1-4.

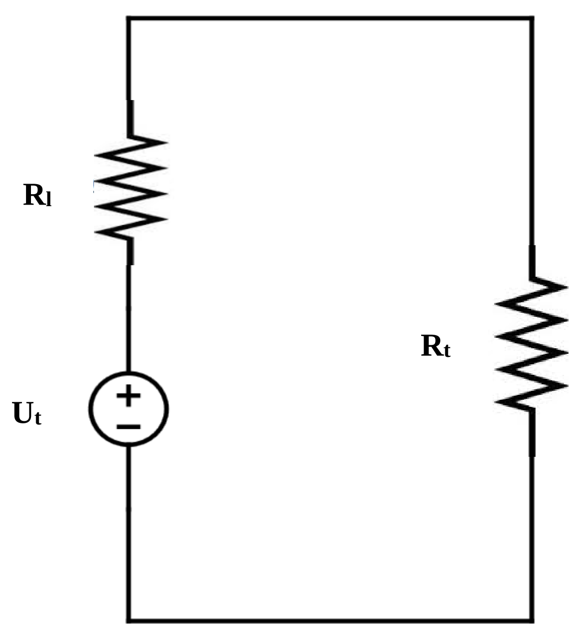

Figure 1-4 Model of original generator circuit

The source of the circuit is the thermoelectric couple that provides the electricity caused by temperature gradients over the thermoelectric unit. It is presented as Ut. The internal resistance of the power source is modeled by the resistor R_t. The load resistor is presented by R_l. As the load resistance varies all the time as the electric load changes, the power output changes value as well. The values of power source and internal resistance are set as constants as they are uncontrollable parameters of thermoelectric generator. Based on ohm's law and other related electric principles and definition, the power output can be derived as following:

$$\begin{aligned} I &= \left(\frac{U_t}{R_t + R_l} \right); \\ P &= I^2 \cdot R_l; \\ P &= \left(\frac{U_t}{R_t + R_l} \right)^2 \cdot R_l; \end{aligned} \tag{1.1}$$

Based on equation (1.1), the system power output depends on the load resistance. In this case, load resistance is the solely variable. The power output is the dependent variable. In order to figure out the changing curve of the power output, derivative of the power output with respect to the load resistance is necessary.

$$\begin{aligned} \frac{dP}{dR_l} &= \frac{d(\left(\frac{U_t}{R_l + R_t} \right)^2 \cdot R_l)}{dR_l}; \\ \frac{dP}{dR_l} &= \frac{U_t^2 (R_t^2 - R_l^2)}{(R_t + R_l)^2}; \end{aligned} \tag{1.2}$$

From the equation (1.2), conclusion can be made easily that the power output approaches its peak value as the load resistance equal to internal resistance of the thermoelectric generator. The power output increasing as the load resistance augmenting before the value approach the internal resistance.

With the circuit demonstrated as show in this figure 1-4, the power output as a function of the load resistance is based on the experimental data, and the parameters are assumed as shown in table 1-1.

Table 1-1 Parameters of original circuit (1)

U_t (V)	R_t (Ω)	R_l (Ω)
16	0.5	0 to 2

Using Matlab to plot the relationship between power output and load resistance, the peak power output, augment and decreasing ratio are demonstrated as below.

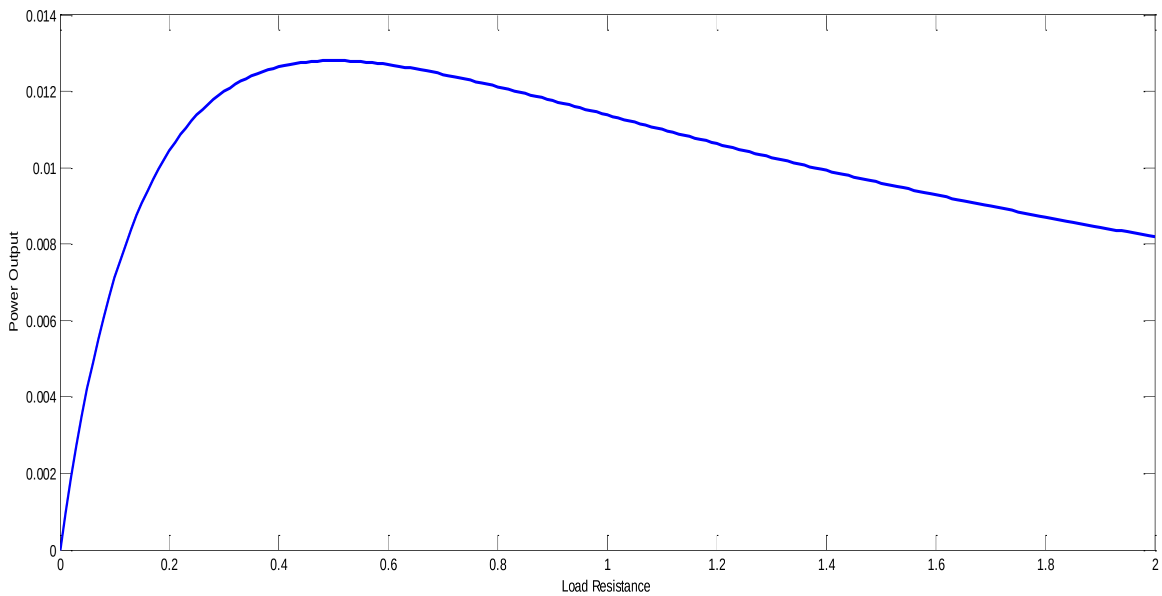

Figure 1-5 Relationship between power output and load resistance

From the plot, it is clearly shown the peak of the power output occurs when the load resistance is equal to the internal resistance of the circuit.

Aiming at comparing the result of the math model of original circuit which consists only basic components as load resistance, internal resistance and electricity source, Matlab/Simulink is used as the core tool for developing circuit model and simulation circuit. In this thermoelectric circuit study, Simscape tool box is used as the modeling tool. Figure 1-6 is the Simscape model of the electric circuit of thermoelectric generator.

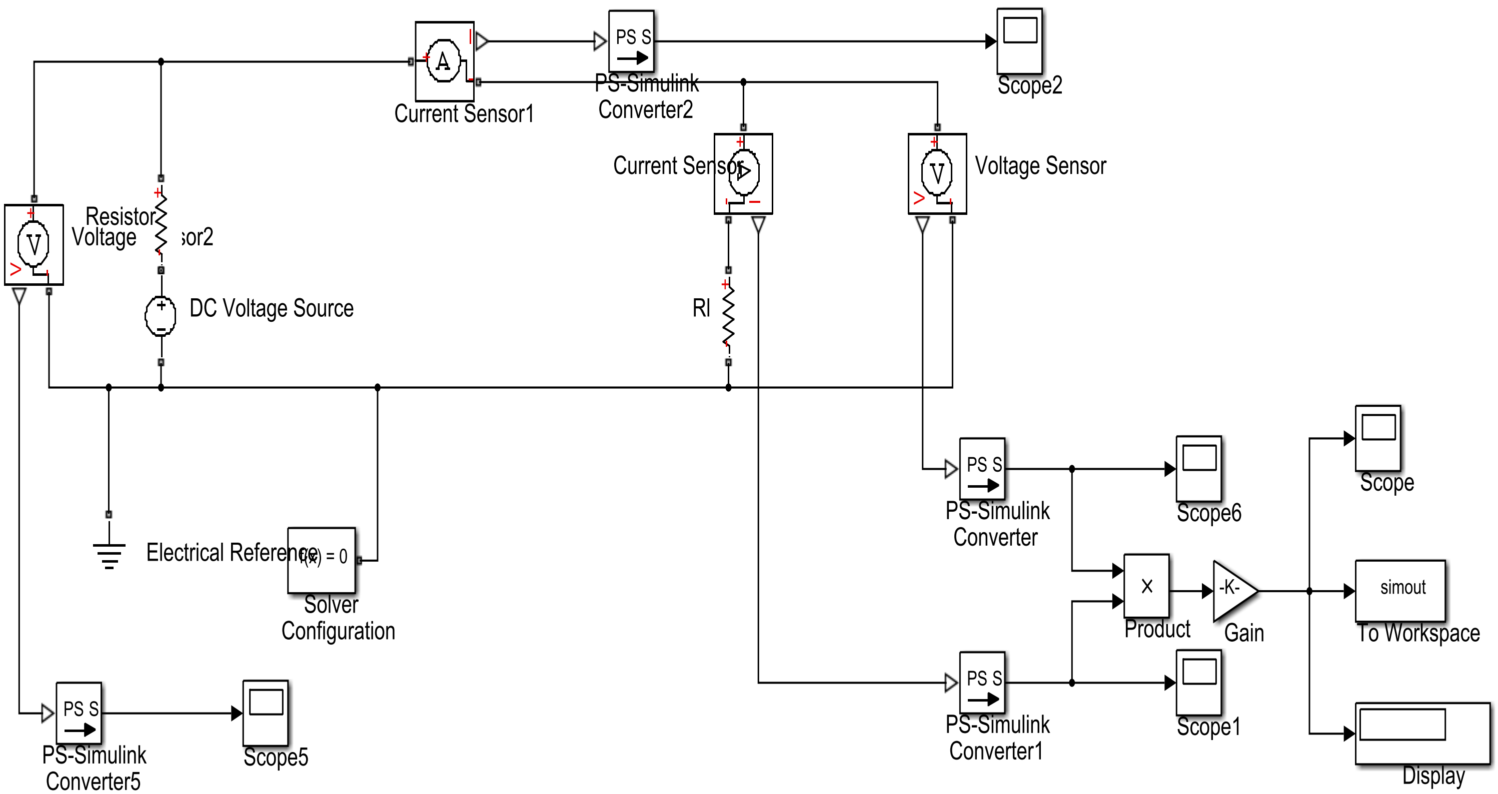

Figure 1-6 Simulation model of original circuit of thermoelectric generation

With some similar process of simulating the circuit result, the relationship curve of analytical and simulation solutions can be acquired and compared with each other. In the process of the comparing, it can easily generate the conclusion that both solutions are identical and match each other very well. Table 1-2 is the parameters used to run for modeling.

Table 1-2 Parameters of original circuit (2)

U_t (V)	R_t (Ω)	R_l (Ω)
16	0.5	0 to 1

Figure 1-7 is the result of comparing of two curves from math model and simulation model.

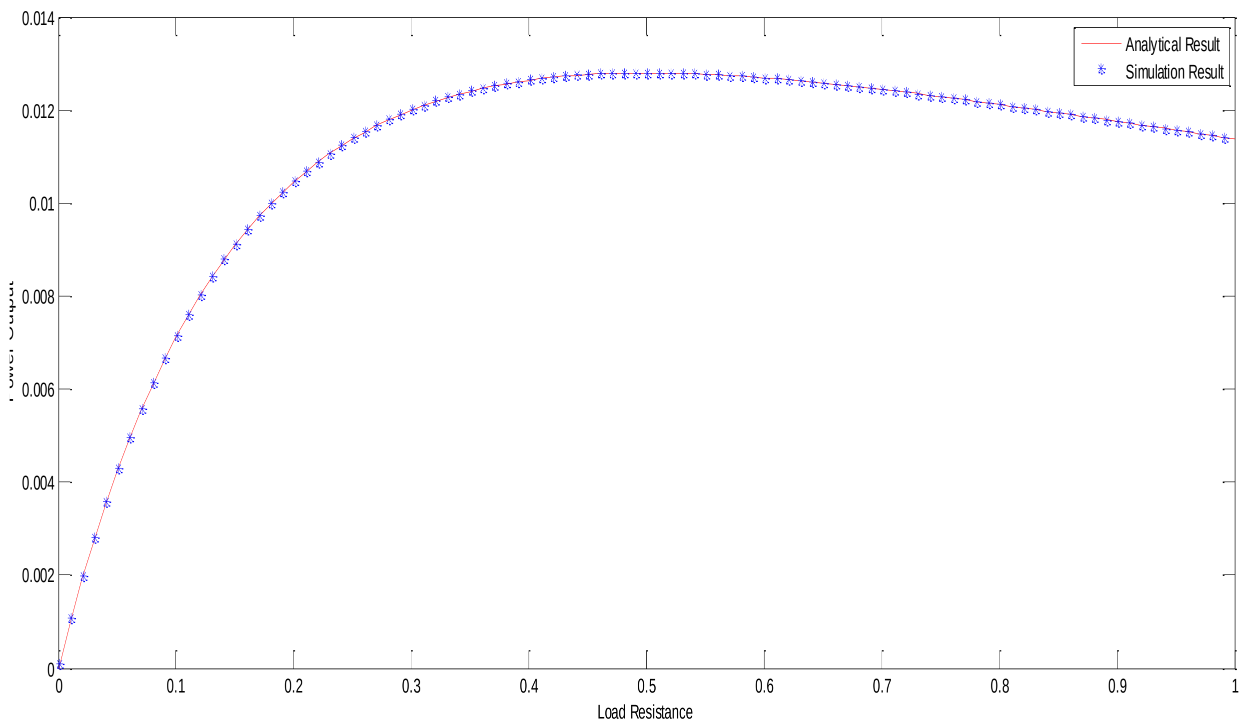

Figure 1-7 Results comparing of the analytical solution and simulation result

From Figure 1-7, it can be seen that the simulation result matches the analytical result perfectly. This is quite a verification process for simulation with Matlab/Simulink. In order to optimize the circuit for the best system perform when the load resistance changes, a controlled switch and two capacitors are introduce in to this system as a buck converter, which play the role of optimizing the system efficiency.

1.2.2 Motivation of Power output Optimization

With the goal to optimize circuit, a circuit has been designed with controlled the duty cycle. The new circuit consists a switch and two capacitor. The two capacitors are paralleled used for storing energy while the power cannot be delivered to the load resistor directly. Duty cycle is used to control the circuit for optimal efficiency. With the controlled duty cycle, even with the changing load resistance value, the circuit can optimized for maximum power. The research involves with studying the control circuit and focuses on configuring the parameters. Mathematical model and matlab Simscape model will also be compared to figure out the simulation accurate. The improved method of the circuit is demonstrated following in figure 1-8.

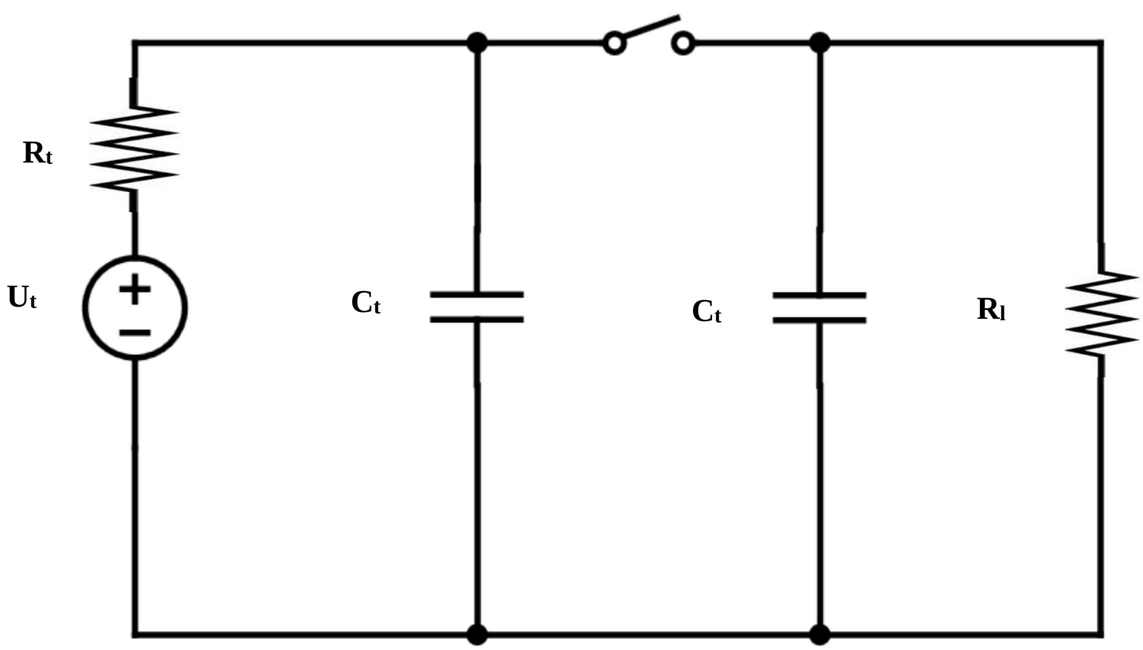

Figure 1-8 Improved circuit with capacitors and switch

This circuit has two working states when the switch opens and closes. The first state is open state. In this working state, the capacitor C_t keeps being charged by the power source. In the meantime, the capacitor C_l supports load resistor R_l alone. In the close state, the switch closes while the whole system is connected. In this state, the power source and capacitor C_t charge load resistor. The percent of close state over the given period is duty cycle. The period is sum of the time open and closed and is determined by control frequency. In our research, 0.0001s is chosen as the period that is equivalent to 10 kHz control frequency. The percent of duty cycle is the control parameter. By adapting duty cycle, the system can be controlled for optimal efficiency with vary load. There are several advantages of the improved circuit compared with the original one without switch and capacitors. With the controlled system, it is possible to deliver more power to the load resistor with low load resistance. This can be proved by simulation results to be introduced later. The simulation of the circuit is shown in figure 1-9.

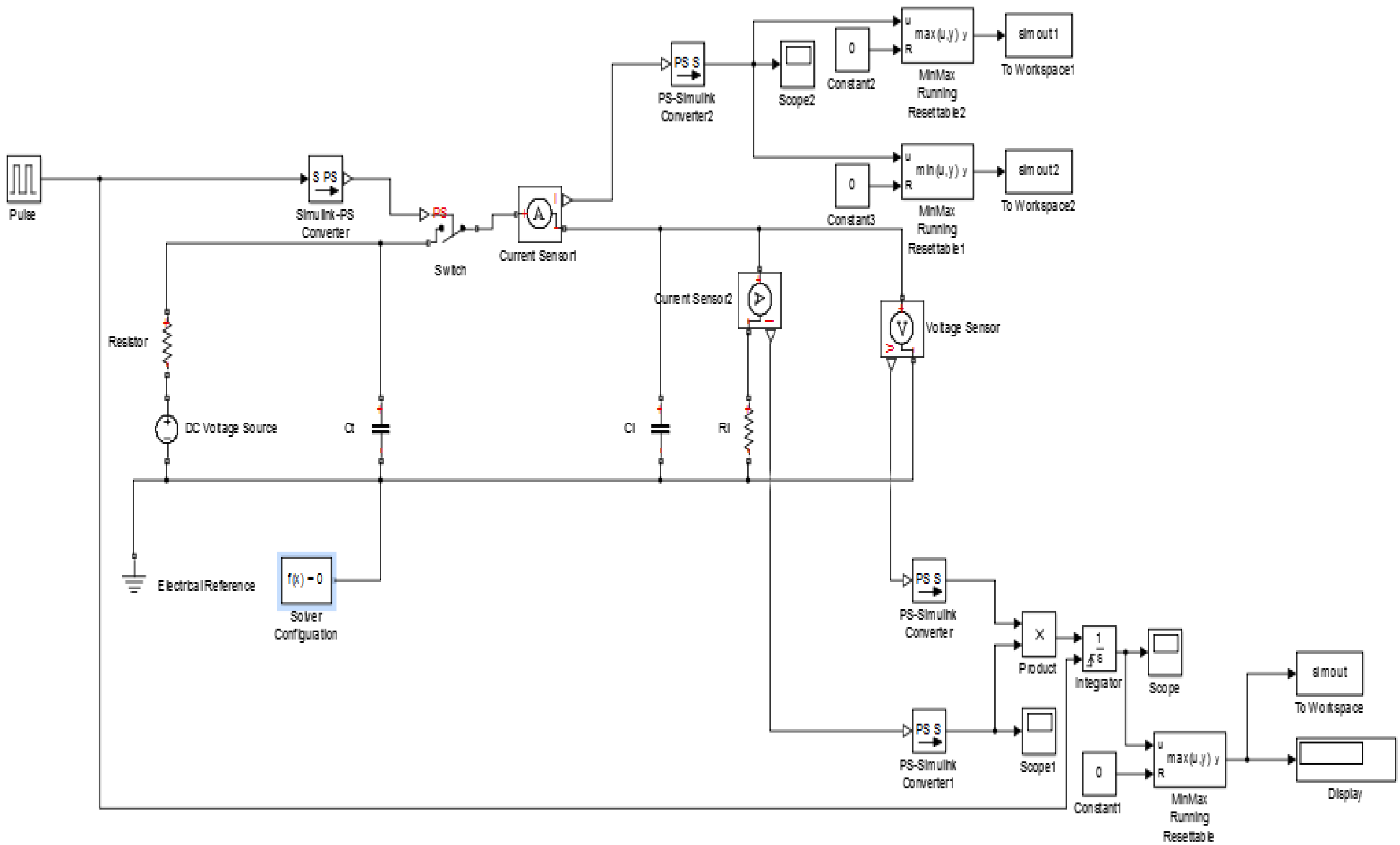

Figure 1-9 Simulation model of improved circuit

By simulating the model of improved circuit, the data of power output with different load resistances can be collected. In order to compare with the power output of the orignial circuit, the same parameter of power source and resistors are chosen for simulation. The parameters of capacitors and controlled duty cycle are list in table 1-3 abd they were optimized in charter 4.

Table 1-3 Parameters of improved circuit (1)

U_t (V)	Ct (F)	Cl (F)	R_t (Ω)	R_l (Ω)
16	400e-6	10e-6	0.5	0.05 to 0.6

The power outputs and load resistance values relationship shown in figure 1-10 demonstrates the power output can be improved over the orignal one.

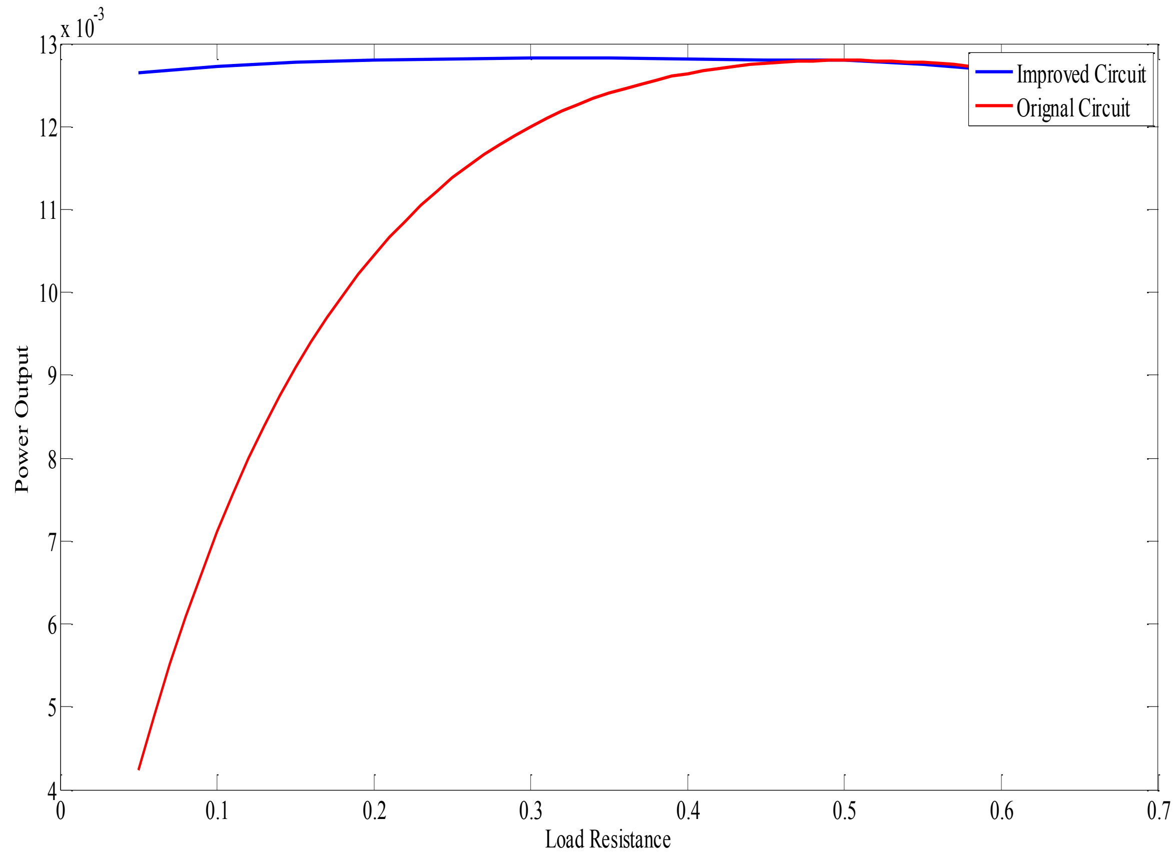

Figure 1-10 Power outputs comparing

From the figure, it can be detected easily that part of the blue curve is above red curve which means that the power output is enhanced in this section. This means even with controling duty cycle, the power output of improved circuit is higher than the original circuit with the load resistance is smaller than 0.6Ω. This motivates the development of the controlled circuit.

1.2.3 Strategy of Circuit Optimizition

By investigating the improved circuit, there are some problems needed to be solved in the improved circuit. The main problem is that at the instant of the switch closing, the current through the swith approaches infinity high. Under the parameters of Table 1-3, simulation results show that the current through the switch approaches 66100 A. the high current could lead to damaged swith or reduce life. Therefore, the simulation results shown in figure1-10 us to study the power output ability. In the following simulation work, the improved circuit model with two capacitors and an inductor is also going to be used as a power output varification.

To solve this problem, buck converter are introduced and utilized in this research as the optimized circuit format.

In order to decrease the current pulse generated by the capacitors at the close moment, an inductor is added between two capacitors. The characteristic of inductor is opposing the change of current which flows through it. It effectively prevent the current changing abruptly. However, as soon as the switch opens, the current flowing though the inductor stops suddently. Due to the characteristic of inductor, the voltage of inductor is the changing rate of current flowing though it self. This abruptly changing of current can make the voltage of the inductor at this time approachs infinity, which is also not faverate in real world application. To cope with this potential problem and also aim at improving power output, a diode is added. The cathod terminal connected between the switch and inductor. The anode is connect to the grounding loop side. With this design strategy, the diode performs as disconnection when the switch is close for the reason that the electric potential over cathode is higher than that over anode because of electric source. The current cannot flow through the diode. The electric source keep charging the capacitors, inductor, internal resistor and load resistor. This state are not affected by the diode added. In the opening case, the diode perform as a wire with slight resistance. The advantages of the new circuit are two folds: the inductor can store certain energy that can contribute to the load resistance power output when the circuit is open; and the current impulse and voltage impulse are significantly reduced. This circuit is a buck converter format. However, as the internal resistance is considerately large, this circuit cannot be classified as a traditional buck converter. The figure 1-11 demonstrated how the final optimized circuit built.

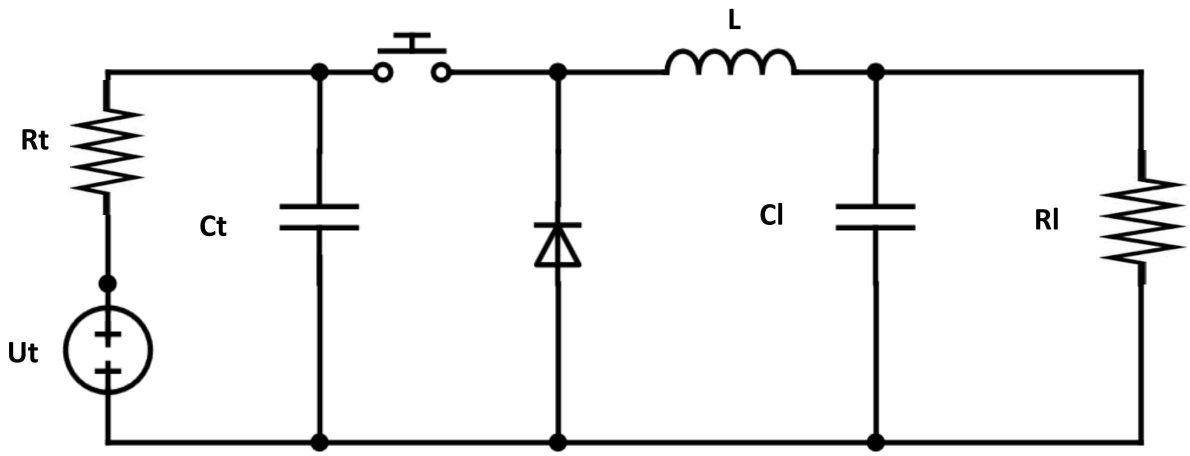

Figure 1-11 Buck converter (1)

Chapter 2 Literature Review

The buck converter is widely used in industry. In this chapter, some outstanding articles about modeling buck converter, buck converter control design and buck converter application are summarized and discussed. These articles are used as the background knowledge to make this thesis easy to read.

2.1. State-Space Average Method

Buck converter is a variable structure system as it has two working status. One working status is closed status. When the switch of the buck converter is closed, the power source charges the other components of the buck converter. The power is delivered from the source power through the switch to the storage electric components and to the load resistor as well. The other working status is open status. In this status, the switch opens and the power is delivered from the storage components to the load resistor. The electric power source is isolated from the load resistor. With this structure feature, a buck converter can be defined as a nonlinear system [6].

To build the mathematic model of the buck converter, regular method of building state-space equations cannot be adopted. The state-space average method can be used as a replacement. The central idea of state-space average method is building the system state-space equations in different work states, respectively. Then, the next step is combining the two state-spaces models in to one state-space model by multiplying their corresponding cycle ratio. The cycle ratio depends on the duty cycle.

For example, regarding the buck converter shown in Figure 1-10, the state-space of the open working state can be modeled as

$$\begin{cases} \dot{x}(t) = A_1 x(t) + B_1 u(t); \\ y(t) = C_1 x(t) + D_1 u(t); \end{cases} \tag{2.1}$$

and the state-space of close working state can be modeled as

$$\begin{cases} \dot{x}(t) = A_2 x(t) + B_2 u(t); \\ y(t) = C_2 x(t) + D_2 u(t); \end{cases} \tag{2.2}$$

The duty cycle time of the buck converter is presented as d and the associated period is T. Thus, the duty cycle of the close working can be calculated as

$$\mu_2 = \frac{d}{T}; \tag{2.3}$$

And the cycle of open working state is

$$\mu_1 = 1 - \frac{d}{T}; \tag{2.4}$$

The new state space model can be generated as

$$\begin{cases} A = \mu_1 \cdot A_1 + \mu_2 \cdot A_2; \\ B = \mu_1 \cdot B_1 + \mu_2 \cdot B_2; \\ C = \mu_1 \cdot C_1 + \mu_2 \cdot C_2; \\ D = \mu_1 \cdot D_1 + \mu_2 \cdot D_2; \end{cases} \tag{2.5}$$

With this state-space average method, a linear state-space model can be obtained even though the target buck converter is a nonlinear system [6]. All the state-space matrices above are for demonstrating. So the specific matrices are not shown here.

However, this method has some disadvantages for building the system mathematic model and it is not adopted in this research. The significant disadvantage is that the response of the linear form state-space model is much different from the actual response of the physical system which oscillating a lot with the oscillated duty cycle input. This makes considerable error comparing with real buck converter system, especially regarding the power output. In this research, the way to build mathematic model is different from this one. The system state-spaces model are not combined into a new. Simscape simulation model and real-time switching state-space model are used in this research. They yields accurate response, compared with the state-space average model method. This will be discussed in Chapter 3 with model comparing.

2.2. Buck Converter Transfer Function

In article [7], Optimum Design of Buck Converter Controller using LQR Approach, a simplified approach of obtaining the buck converter transfer function was introduced. The sample buck converter is shown as following.

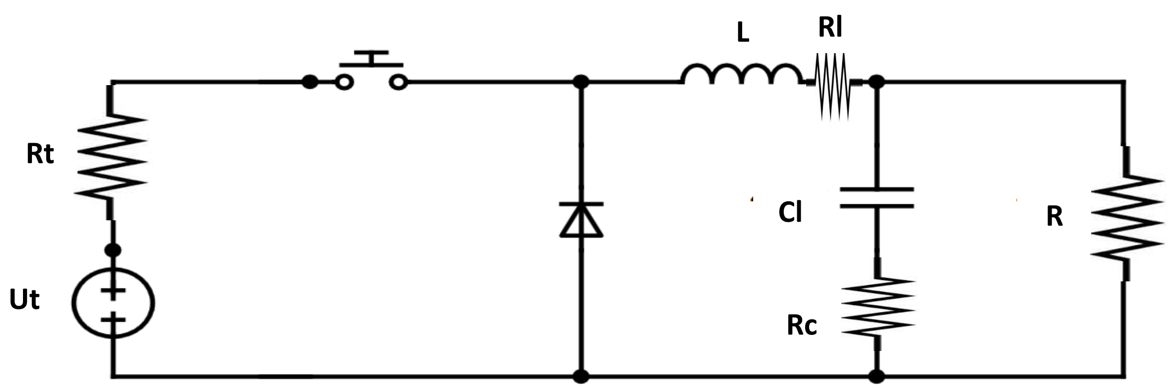

Figure 2-1 Buck converter (2)

In this article, the way to build the overall buck converter transfer function is building the transfer function of the system in closed working state and using it as the overall transfer function. The effective voltage is the source voltage multiplies the duty cycle. The result transfer function is

$$G(s) = \frac{R + R \cdot R_c \cdot C \cdot s}{(LC(R+R_c))s^2 + (L + R_l CR + R_l CR_c + RR_c C) \cdot s + (R + R_l)}; \qquad (2.6)$$

This transfer function is proved to work relatively well [7] for relatively small internal resistor R_t. In this research, the internal resistance is not small and cannot be neglected. On the other hand, the buck converter designed in our research contains another capacitor C_t close to the power source for storing energy when the switch is open. The effect of this capacitor cannot be ignored also. For these reasons, building transfer function in this way is not suitable for our research.

2.3. Pulse Frequency Modulation

In many fields of industries, stable constant power sources are required. Linear supply device can meet this goal with the disadvantage that some energy is wasted when it is delivered through some passive elements. Switch regulators have advantages on this aspect rather than linear supply regulator. Switch regulators can be classified into two types: PFM (Pulse Frequency Modulation) and PWM (Pulse Frequency Modulation) [8].

PFM is selected frequently in the applications that needs to be considered to provide very low stand-by currents. The PFM is applied in the application with light load also. In this model, the way to control the buck converter switch is controlling the frequency of the switch with a fixed duty cycle width [9].

There are several features with the PFM when it is applied to a buck converter. The switching frequency is usually low compared with other pulse modulations. It will yields relatively larger voltage ripple due to this reason. PFM buck converter is also relatively hard to be assessed as the light load needs discontinuous conduction model.

In our research, the PFM is not selected for controlling target buck converter due to high stand-by current of the thermoelectric generator. In order to reduce the ripple, a high frequency switch control is preferred in this research.

2.4. Pulse Width Modulation

PWM (pulse width modulation) is the method selected in this research. There are many reports and researches about PWM. The way of controlling buck converter by PWM is to turn on and of the switch with varying duty cycle at a fixed frequency.

PWM buck converter performs quite well when it working with high load. The power output is high and the ripple is reasonable. However the light load is not the working range of PWM. The ordinary working frequency of the PWM is 200 KHz t0 2 mHz. With this frequency, the energy lost in switch part is quite high and cannot be neglected when the load is a small. However in this research, the resistance of the switch is small enough to be neglected as it compared with the load resistance.

Some design methods are also studied in order to find a modulation that combined the advantages of PFM and PWM. A study about applying a high efficiency PWM with a novel DCM (discontinuously-conducting-mode) on buck converter reports that the buck converter can be controlled to perform well under both high and light load. The size of controller and the performance of the buck converter are both outstanding as shown in Figure 2-2. The block I_L

detector and Mode -control circuit do not work with the current through the inductor is positive. Once the I_L detector detects the current is under zero, these two blocks will switch the buck converter from regular mode to DCM mode [10].

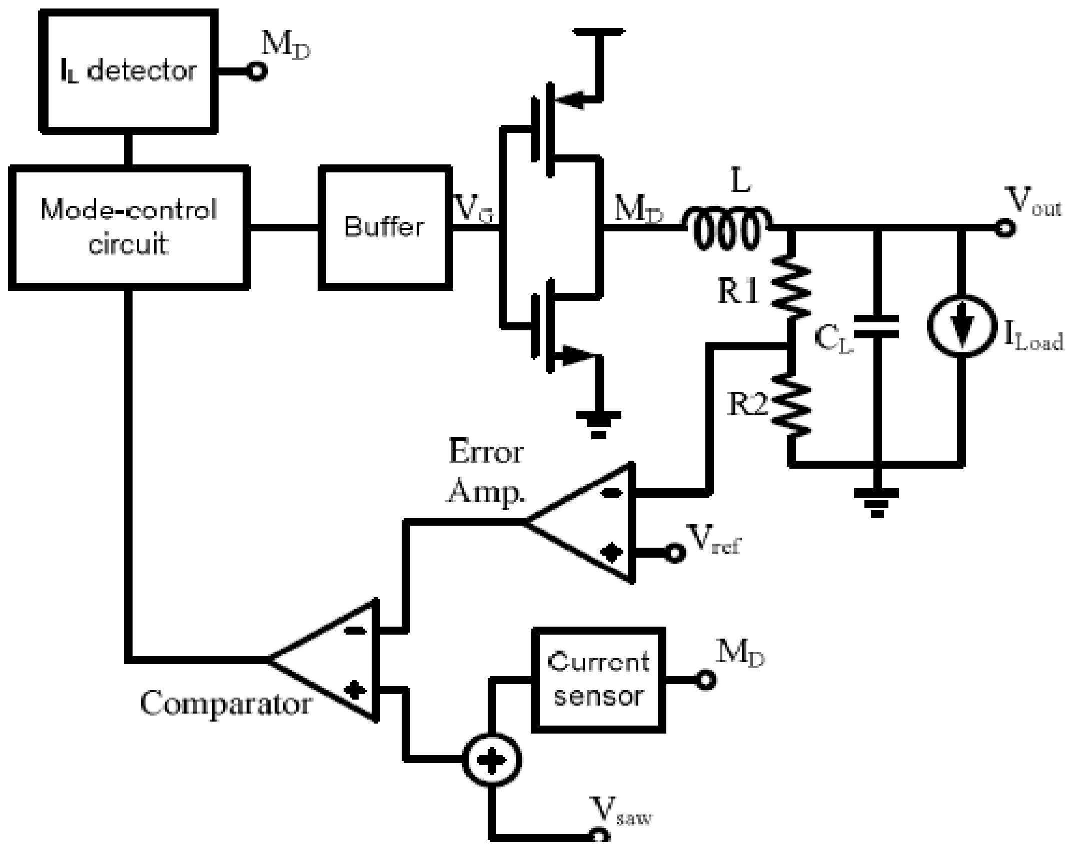

Figure 2-2 Proposed PWM Buck Converter

(A High-Efficiency PWM DC-DC Buck Converter with a Novel DCM Control under Light-Load, Chu-Hsiang Chia**)**

2.5. PID Controller

As the most widely used controller, PID (proportional-integral-derivative) controller is also used in buck converter area. There are many researches about applying PID controller into the buck converter. To improve the control performance, some advanced theories are applied in the research.

2.5.1. Fuzzy logic Control

Fuzzy logic based PID controller was also used to control the buck converters when the performance of PID controller cannot meet the requirement in some aspects. By employ fuzzy logic based PID controller, the performance can be improved. The process of fuzzy logic contains two parts: fuzzification and defuzzification. The first part can be demonstrated in this way: converting probabilistic data into fuzzy value. The second part of defuzzification is applying the membership functions on the input data and yielding output in a form of specific value. Regarding this scheme, the specific mathematic model of target system is not necessary. This characteristic of fuzzy logic method is very feasible for building controller for some nonlinear system like buck converter [11]. According the research in [11], the result of the fuzzy logic based PID controller is far better than a conversional PID controller for controlling buck converter. The relative research report in [12] also introduced fuzzy logic PID controller in a concisely experimental way.

2.5.2 LQR Approach

LQR (linear-quadratic regulator) is widely used in controller design. In research report [7], LQR are used for figuring out the feedback signal to tune PID gains in a buck converter. By building the cost function of the buck converter system, the optimum gain vector is acquired. With this vector, the PID gains can be tuned. These three gains are used for tracking the reference signal with reduced error. These gains forms the optimum gain vector.

2.6 Sliding Mode Controller

Sliding mode control is a control method for nonlinear system. When it is applied to a structure variable system buck converter, there are several advantages of using sliding mode method to design controller. The sliding mode controller is insensitive to external disturbance for its outstand robustness. It also has fast response ability and good transient performance.

The way to select variables for buck converter system is different from the conventional way to build differential equations of the circuit system. The variables selected are not the physical values as the voltages of capacitors or currents through the inductors. The variables are selected as the output voltage error, differential of this voltage error and its integral [13].

Regarding selecting the sliding surface that trajectories are going to converge to, research reported in [14] made a good explanation on this part. Only getting the inequities which defined the range of sliding coefficient is not enough for getting a good coefficient. To figure out the coefficient, Ackermann's Formula for designing static controllers is adopted. Regarding specific problem on designing controller for buck converter, the bandwidth of the desired frequency response in conjunction with the existence condition are the key elements.

2.7. Conclusion

As a widely used switching regulator, buck converter is combined with many advanced control theories. Sample data feedback [15], optimal control theory [16] and double-frequency buck converter [17] are all relative technologies about buck converter control. The control theory adopted in this research is extreme seeking control. This is going to be introduced further in Chapter 5.

Chapter 3 Analytical Analysis and Simulation

To study the circuit and the associated control design for the buck converter, developing simulation model is necessary. Especially in this research, some models are not able to be realized in real experiments but it can be simulated in software. The parameters and strategies, even for some extreme cases, can be easily acquired or verified by simulations without building the physical system. In this chapter, the emphasis is focused on developing both analytical model and Matlab simulation model for the circuit. The modeling accuracy is validated by comparing their simulation results.

3.1. Mathematic Analysis of Circuit Model

In this section, the mathematic analysis of circuit model is introduced and demonstrated. In fact, in chapter 1, the mathematic method of original circuit has already been show and the result is utilized to optimize circuit into buck converter format. There are two mathematic models introduced in this section. The first one is analytical model of the improved circuit. This circuit is consisted with electric source, internal resistor, load resistor, switch and two capacitors as shown in figure 1-8. The second one is the optimized circuit with added inductor and diode in the improved circuit as shown in figure 1-11. The advantages of the mathematic analysis of circuit models are: the circuit can be processed more accurately and efficiently; controller design can be conducted more logically and clearly. With the foundation of mathematic model developed in this section, verification simulations model is more readily and impressively.

3.1.1. Mathematic Model of Primarily Improved Circuit

In order to conduct the analysis of the primarily improved circuit mathematically, it is necessary to analyze the circuit as the first step. As mentioned in Chapter 1, there are two working states of the circuit within one period. The first state is the open case. The second state is named as closed case. In figure 3-1, the open case work state is shown, the whole circuit is divided into two parts. The left part is consisted by the power source, internal resistor and capacitor C_t. As the electric source U_t and internal resistor R_t are defined as constants, the whole part A circuit can be seen as a standard capacitor charging circuit. In the meantime, the part B circuit can be seen as a capacitor discharging circuit.

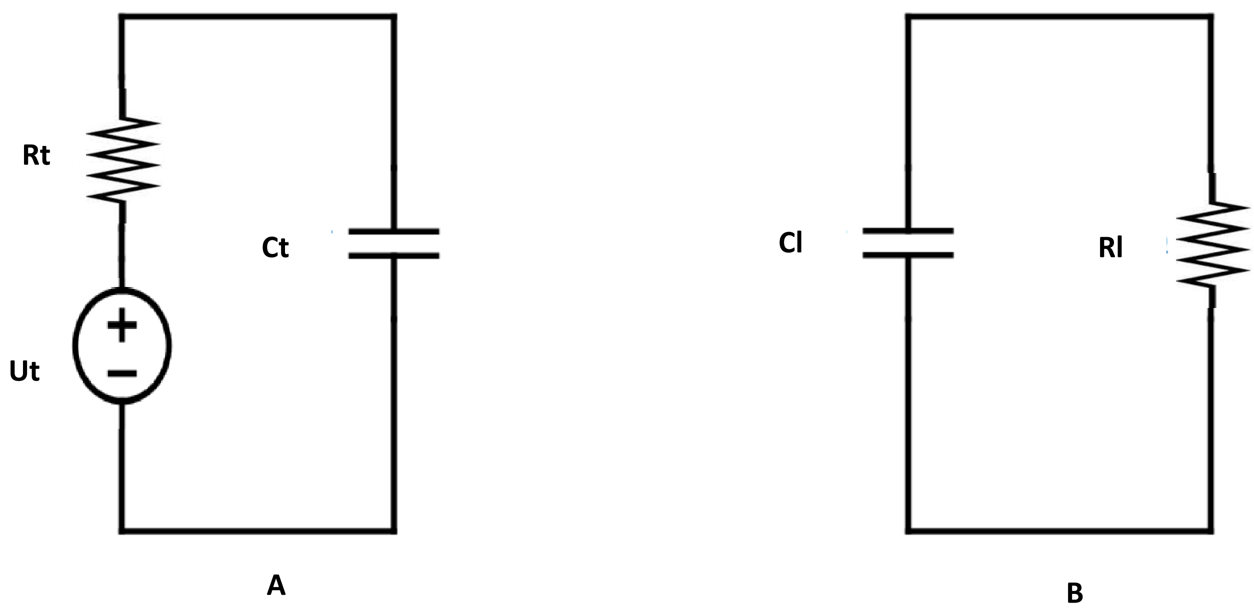

Figure 3-1 Open state of the primarily improved circuit

Regarding the part A and part B circuits, building mathematical solution requires to clarify initial conditions of these two circuits. To research this goal, the whole system is analyzed over a control period. Note that at the steady-state initial voltages of capacitors at the instant of the switch opening are equal to the voltages at the end of the last closed case. Regarding the closed case, two capacitors are connected in parallel. The voltages of parallel capacitors are equal according to the principle of electric circuit. Further considering this circuit structure, a conclusion can be made that the initial voltages of two capacitors are equal to each other. U_0 are used to represent for the initial voltages of capacitors.

$$I_{C_t} = \frac{(U_t - U_0) \cdot e^{-\frac{t}{R_t \cdot C_t}}}{R_t}; \tag{3.1}$$

$$U_{C_t}(t) = \frac{1}{C_t} \cdot \int_0^t I_{C_t}(\tau) d\tau + U_0; \tag{3.2}$$

These two equations (3.1) and (3.2) are the mathematic equations of charging capacitors which has initial voltage from the part A circuit. The solution of these two equations are shown below.

$$U_{C_t}(t) = U_t + U_0 \cdot e^{\frac{-t}{(R_t \cdot C_t)}} - U_t e^{\frac{-t}{(R_t \cdot C_t)}}; \tag{3.3}$$

In the meantime, part B circuit is also working as a capacitor being discharged. The equation of this circuit is shown like this.

$$I_{C_l} = \frac{-U_0}{R_l} \cdot e^{\frac{-t}{R_l \cdot C_l}}; \tag{3.4}$$

$$U_{C_l}(t) = \frac{1}{C_l} \cdot \int_0^t I_{C_L}(\tau) d\tau + U_0; \tag{3.5}$$

(3.4) and (3.5) are two equations that describes the process of discharging capacitor in part B circuit. The solution of these set of equations are shown below.

$$U_{C_t}(t) = U_0 \cdot e^{\frac{-t}{R_l \cdot C_l}}; \tag{3.6}$$

With equation (3.3) and (3.6), the capacitor voltage as a function of time t during opening case can be obtained easily. Based on these equations, capacitor voltage can be obtained for the opening case working state.

Regarding the closed case working state, the same method can be applied to the circuit. The initial condition of the circuit comes first to be considered. Because of the parallel connection, a new capacitor can be the equivalent of these two capacitors. Figure 3-2 shows this transformation.

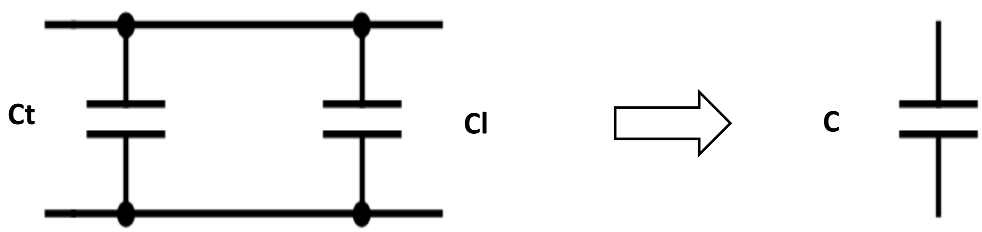

Figure 3-2 Capacitors transformation

The combined capacitance of new capacitor can be calculated as shown below.

$$C_t + C_l = C; \tag{3.7}$$

At the instant of closing the switch, the two capacitor's voltage has to be equal as they are parallel. However the electric charges of these two capacitors cannot be transferred instantaneously. So the electric charge energy in two capacitors are conserving in this instant. According to the conservation of charges, the voltage U_c of new formed capacitor C can be get as the following equations. Assumes that the time of open case work state is t_1.

$$U_{C_t}(t_1)\cdot C_t + U_{Cl}(t_1)\cdot C_l = U_c \cdot C; \tag{3.8}$$

$$U_c(0) = \frac{U_{C_t}(t_1)\cdot C_t + U_{C_l}(t_1)\cdot C_l}{C_t + C_l}; \tag{3.9}$$

The next step is simplifying the resistors of the circuit. According to Thevenin's resistance theorem, when a single resistance can replace a set of parallel resistors, and the voltage source is also treated as a short circuit. In this way, the new resistor can be formed to replace the parallel resistors as shown in Figure 3-3.

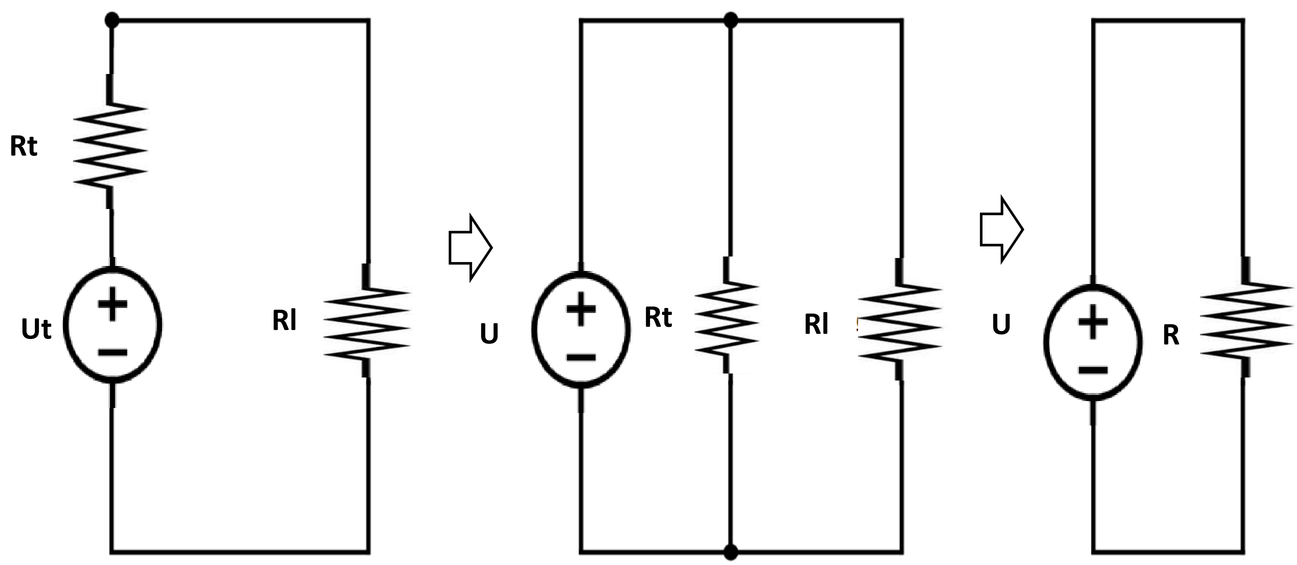

Figure 3-3 Capacitors transformation

With these following equations, the resistance are worked out.

$$R = \frac{R_t \cdot R_l}{R_t + R_l}; \tag{3.10}$$

Also according to the Thevenin's voltage source theorem, the new voltage can be calculated as following.

$$U = \frac{R_l}{R_t + R_l} \cdot Ut; \tag{3.11}$$

By transforming capacitors and simplifying resistors, a new circuit is generated as the Figure 3-4 shown below.

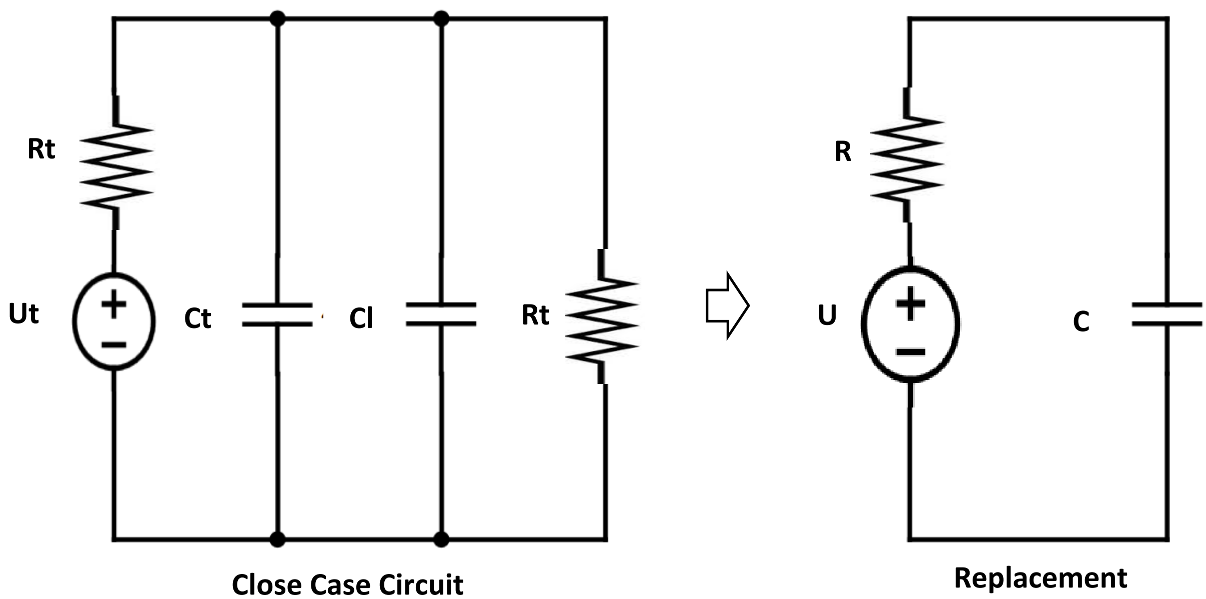

Figure 3-4 Simplification of close circuit

According to this new formed circuit and its initial voltage, the voltage of the capacitor C for the closed case can be acquired easily by solving following equations.

$$I_C = \frac{[U - U_c(0)] \cdot e^{-\frac{t}{R \cdot C}}}{R_t}; \tag{3.12}$$

$$U_C(t) = \frac{1}{C} \cdot \int_0^t I_C(\tau) d\tau + U_c(0); \tag{3.13}$$

After solving the set of equations above, the voltages capacitor of C for the closed case can be shown as follows.

$$U_c(t) = U_c(0) \cdot e^{\frac{-t}{R \cdot C}} - U \cdot e^{\frac{-t}{R \cdot C}} + U_c(0); \tag{3.14}$$

As a periodic system, the voltages of capacitors also varies periodically. Also as the discussion about the initial voltages of open case, the voltages of capacitors at the end of closed case are the same as the initial voltages of open case. T and t_1 are defined as the period and length of open case. Thus, the duty cycle is T-t_1.With time length t_1 and T-t_1, the closed case end voltage and open case initial voltage can be expressed as follows.

$$U_C(T - t_1) = U_{0;} \tag{3.15}$$

By solving this equation, expression of U_0 can be obtained as well. Substituting the expression of U_0 into equation (3.3) and (3.14), all capacitor voltages during a period can be presented with only one variable t_1 (duty cycle), as the length of open case.

Next, regarding figuring out the relationship between power output and duty cycle, is to be studied, along with the power expression of load resistance is the next. As the capacitor C_l is parallel connected with load resistor, the voltage of C_l can be used as the voltage of R_l. In this way, the expression of load resistor power output can be derived as following.

$$P_1 = \frac{[U_l(t)]^2}{R_l}; \qquad KT \le t \le KT + t_1 \tag{3.16}$$

$$P_2 = \frac{[U_c(t)]^2}{R_l}; \qquad KT + t_1 < t < (K+1)T \tag{3.17}$$

As the goal is to control the duty cycle, it is important to figure out the transient power output and the power output over a period as a function of the duty cycle. For this reason, the work done over a period is described in following. It is also calculated in two steps as there are both open and closed cases.

$$W_1 = \int_0^{t_1} P_1 dt; \tag{3.18}$$

$$W_2 = \int_0^{T-t_1} P_2 dt; \tag{3.19}$$

The work done over one period is shown below.

$$W = W_1 + W_2; \tag{3.20}$$

Note that the work is only a function of t_1. By controlling t_1, the work of W can be regulated.

In order to study the relationship curves, a matlab script is developed to simulate these equations. It can be seen in Appendix. Table 3-1 shows the parameters used in simulations. By running this program, a curve is generated to show the relationship between duty cycle and power output. The parameters are selected based by try and error.

Table 3-1 Parameters of improved circuit (2)

U_t (V)	T (s)	C_t (F)	C_l (F)	R_t (Ω)	R_l (Ω)
16	0.0001	150e-6	20e-6	0.5	0.2

According to the parameters offered from table 3-1, running the program generates the curve shown in Figure 3-4. From this figure, it is obviously that while the duty cycle is between 30 to 60 percent, the power output over a peroid approachs to its peak. To calculate this peaking power output and the corresponing duty cycle, a new matlab script is developed. The duty cycle that can give out most power output is at 53 percent of the whole period. Within the original circuit, the same resistance of load resistor can only generate around 0.01024 J work in 0.0001s, which is smaller than the peak power calculated by manually at 0.0113J. One observation is that there is considerable power output at the 0 percent duty cycle point where the power out put supposed to be zero. Considering the primarily improved circuit studied, there is a untoleratable high current flow though the switch at closing,causomg the voltage reset on both capacitors. This might be the reason why there is power output even if the duty cycle approaches zero. The current impulse delivers significantly power to the C_l and load resistor at the time of switch closing. This makes the circuit cannot be used in practice.

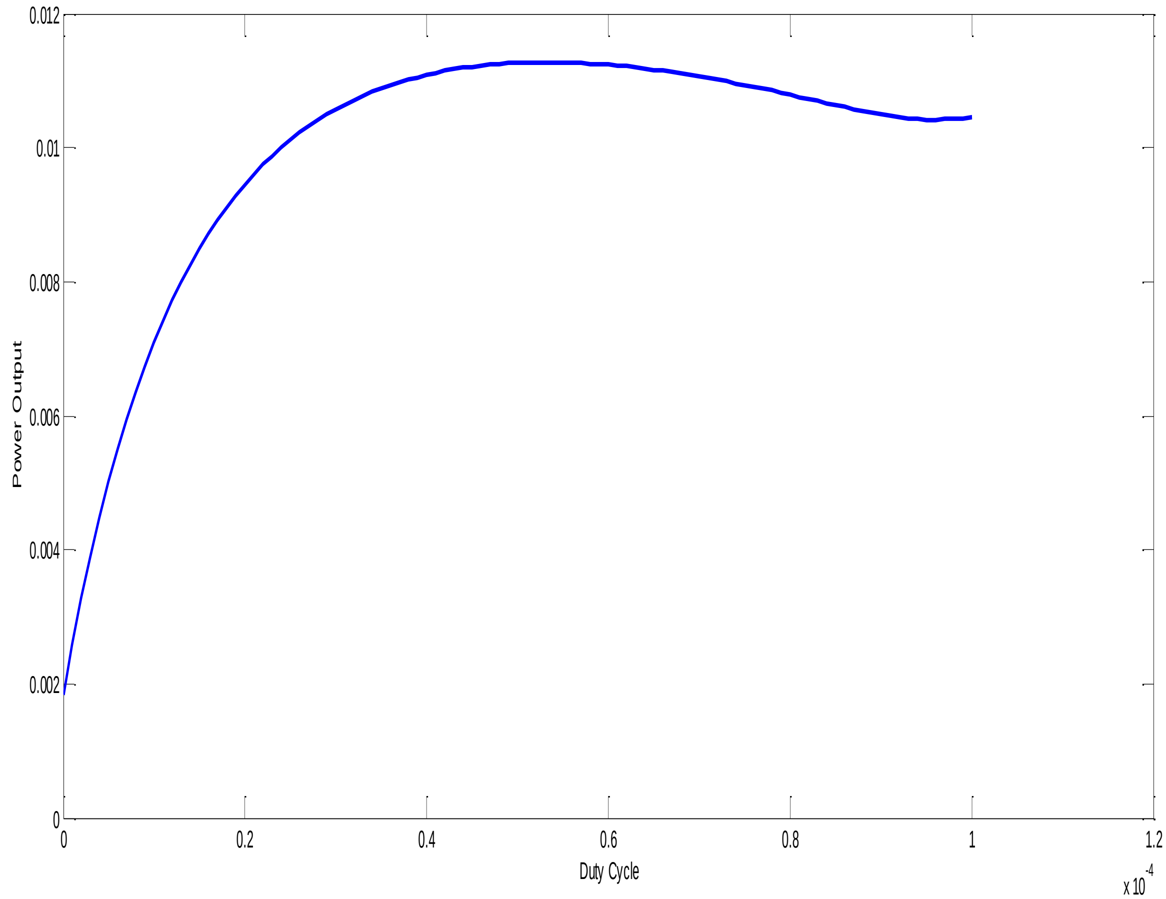

Figure 3-5 Analytical solution of primary circuit

3.1.2 Mathematical Model of the Buck Converter

In this section, the target is to study the final optimized circuit, a buck converter circuit, which is feasible to be built in real experiment. The structure of the optimized circuit is different from the primarily improved circuit with added inductor and diode in to it. With the same method, the differential equations cannot be founded as easy as the primarily circuit for the reason that the buck converter contains nonlinear component rather than primarily improved circuit. To deal with this issue, developing state space model is a good way. Figure 1-11 presents the buck converter to be studied.

To build the state space model of the buck converter circuit, two work states need to be separated. Similar to the primarily improved circuit, there are two work states, closed state and open state. In order to keep researching consistently, the open state is first to be studied. Figure 3-6 is the open state buck converter. There are also two parts in this circuit, part A and part B.

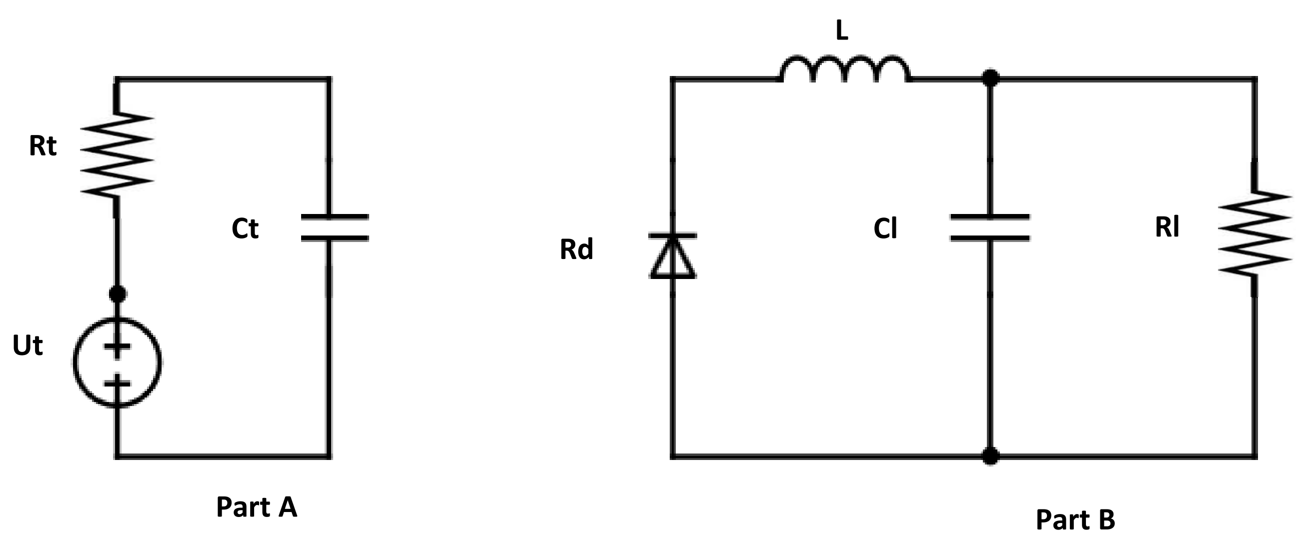

Figure 3-6 Open case circuit

The part A is almost the same as the one in the primarily improved circuit. However the part B circuit is much different from the former one. The voltages of capacitor C_t and C_l are defined as x_1

and x_3 as well the current through the inductor L is x_2. As there is only one capacitor in part A circuit, it is quite simple to build its state space based on Kirchhoff law.

$$U_t = I_{Rt} \cdot R_t + x_1; \tag{3.21}$$

$$\dot{x}_1 = \frac{1}{C_t} \cdot x_1; \tag{3.22}$$

Based on the circuit equation above, the state space of part A is shown below.

$$\dot{x}_1 = -\frac{1}{R_t \cdot C_t} x_1 + -\frac{1}{R_t \cdot C_t} U_0 \tag{3.23}$$

Regarding the part B circuit, the diode is a nonlinear component of the circuit which increases the complication of the building state space model. In this circuit, the diode is modeled to allow a current flow in one direction. In this case, the diode has the same effect of a nonlinearly varying resistor that depends on the voltage over the diode. Once the voltage is less than a certain voltage, the resistance approaches infinity. Otherwise, the resistance approaches zero.

To make the resistance of diode even more accurate, the voltage-current characteristic curve was sketched based on the Physicist's model shown below.

$$I = I_0(\exp\{\frac{eV}{kT}\} - 1); \tag{3.24}$$

In this equation, *I* is the current through the diode; *V* is the voltage over the diode. *T* is the temperature in Kelvin; *e* is electron charge $1.602*10^{-19}$C; *k* is Boltzmann's constant

$1.38*10^{-23}$ J/K.

With selected parameters in the above equation, a curve of voltage current (V-I) for the diode model can be sketched and shown below.

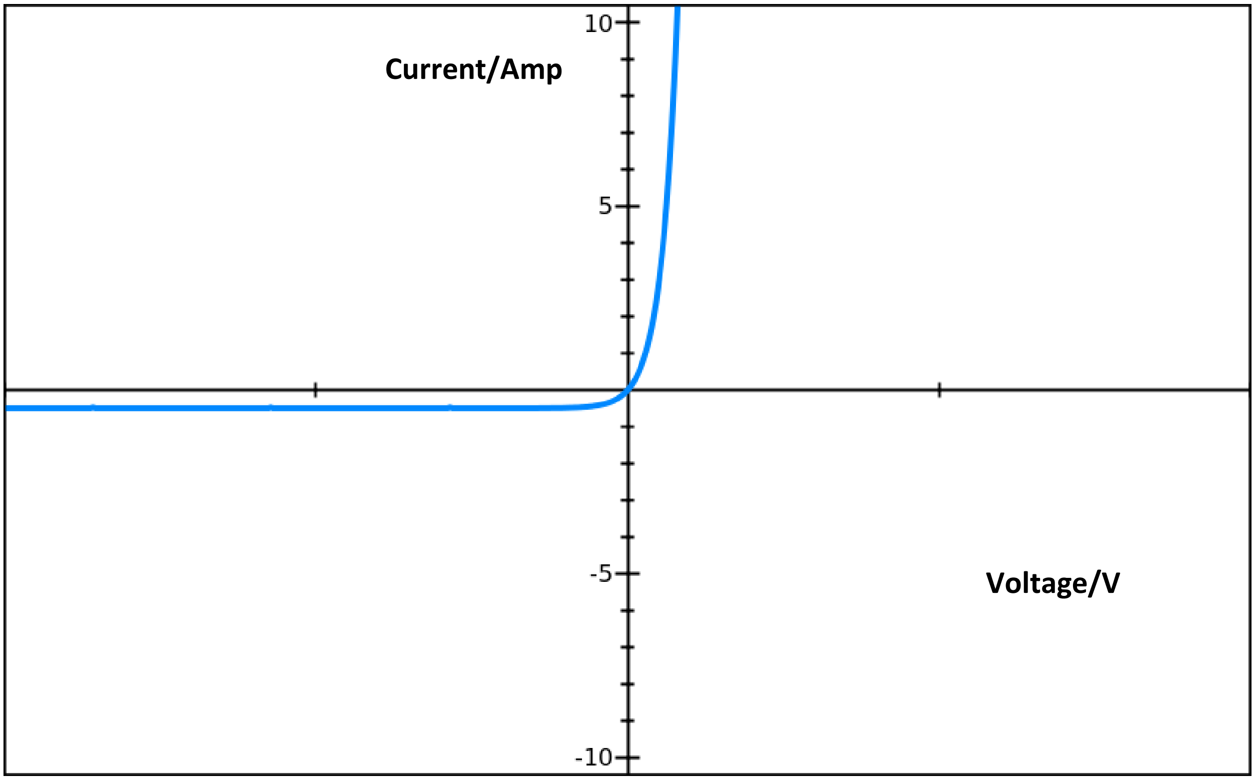

Figure 3-7 I-V characteristic of semiconductor diode

By changing the coordinates, here comes the V-I characteristic of semiconductor diode can also be shown in Fig 3-8. The tangents of the V-I imply the resistance value corresponding to the current. According to Fig 3-8, the differential resistance of this diode varying for infinity large to ignorable small with the current increasing from negative value to considerable positive value. The method adopted in this research is to collect the data of resistance under different voltage values. Based on this data set, a look-up table can be developed. Based on this table, the curve of diode resistance can be founded. The state space simulation are developed using this block structrue.

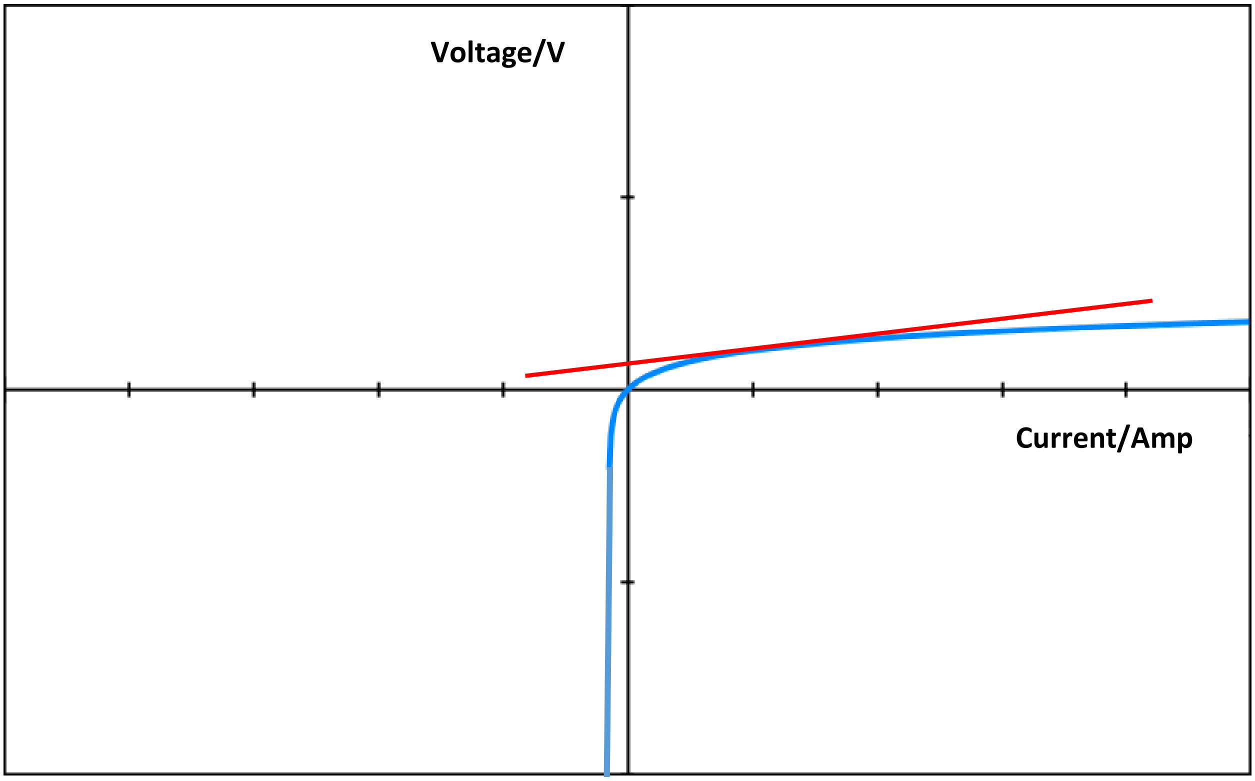

Figure 3-8 V-I characteristic of semiconductor diode

However, before implementing the state space model into Simulink, R_d are defined as the changeable resistance of diode.

The differential equations of part B can be shown below.

$$L \cdot \dot{i}_l + R_d \cdot i_l + U_{C_l} = 0; \tag{3.25}$$

$$i_l = C_l \cdot \dot{U}_{C_l} + \frac{U_{C_l}}{R_l}; \tag{3.26}$$

The state space of this circuit is shown below.

$$\begin{aligned} L \cdot \dot{x}_2 &= -R_d \cdot x_2 - x_3; \\ x_2 &= C_l \cdot \dot{x}_3 + \frac{x_3}{R_l}; \end{aligned} \tag{3.27}$$

Combining equations of (3.23) and (3.27), the state space model is shown below.

$$\begin{Bmatrix} \dot{x}_1 \\ \dot{x}_2 \\ \dot{x}_3 \end{Bmatrix} = \begin{Bmatrix} -\frac{1}{R_t \cdot C_t} & 0 & 0 \\ 0 & -\frac{R_d}{L} & -\frac{1}{L} \\ 0 & \frac{1}{C_l} & -\frac{1}{R_l \cdot C_l} \end{Bmatrix} \cdot \begin{Bmatrix} x_1 \\ x_2 \\ x_3 \end{Bmatrix} + \begin{Bmatrix} \frac{1}{R_t \cdot C_t} \\ 0 \\ 0 \end{Bmatrix} \cdot U_t \tag{3.28}$$

After modeling the circuit for open state, the closed state circuit can be modeled in the same way. The close state circuit is shown as in figure 3-9.

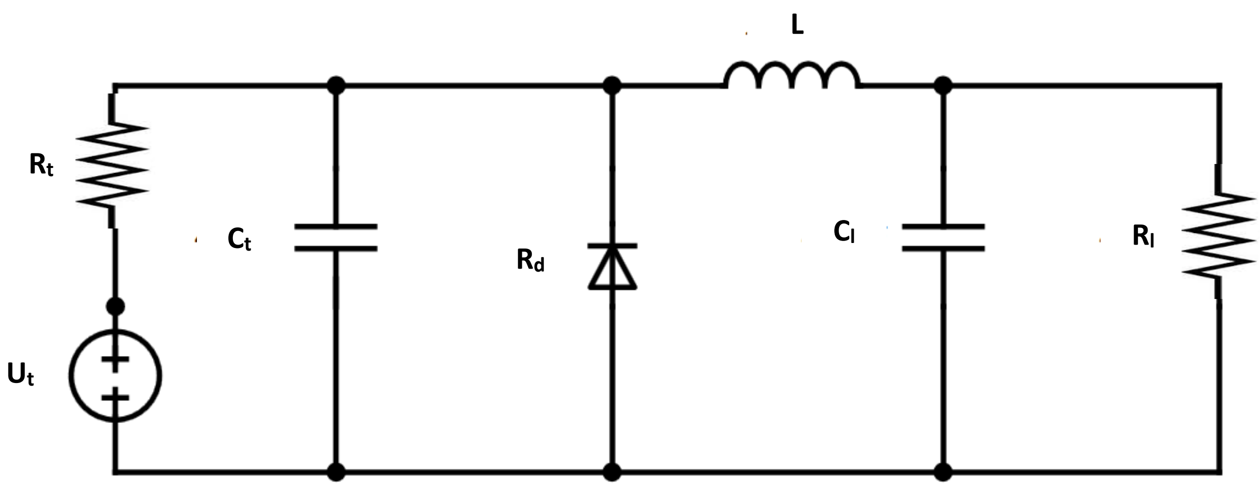

Figure 3-9 Closed state circuit

In this case, because of the power source is connected to the main circuit, the voltage and current relationship can be modeled as following.

$$I_{R_t} = I_{C_t} + I_L \tag{3.29}$$

$$I_{R_t} \cdot R_t + U_{C_t} = U_{0;} \tag{3.30}$$

$$I_L = I_{C_l} + \frac{U_{C_l}}{R_l}; \tag{3.31}$$

Denoting the x_1, x_2 and x_3 in the same way as the open state, the state space model of closed circuit can be founded as follows.

$$\begin{Bmatrix} \dot{x}_1 \\ \dot{x}_2 \\ \dot{x}_3 \end{Bmatrix} = \begin{Bmatrix} -\frac{1}{R_t \cdot C_t} & -\frac{1}{C_t} & 0 \\ \frac{1}{L} & 0 & -\frac{1}{L} \\ 0 & \frac{1}{C_l} & -\frac{1}{R_l \cdot C_l} \end{Bmatrix} \cdot \begin{Bmatrix} x_1 \\ x_2 \\ x_3 \end{Bmatrix} + \begin{Bmatrix} \frac{1}{R_t \cdot C_t} \\ 0 \\ 0 \end{Bmatrix} \cdot U_t \qquad (3.33)$$

Matlab/Simulink is selected as the tool for simulation study in this research. To implement the models in (3.28) and (3.33), the crucial part of the system is to model the switching part. Duel to the buck converter design, there is no voltage collision at switch. The voltages and currents related to the inductor and capacitors are transient. With this conclusion, the system can be treated as that the time responses at the ending of last working state is the initial conditions of the system in the current working state. The time length of each system working state is the duty cycle multiple to the period.

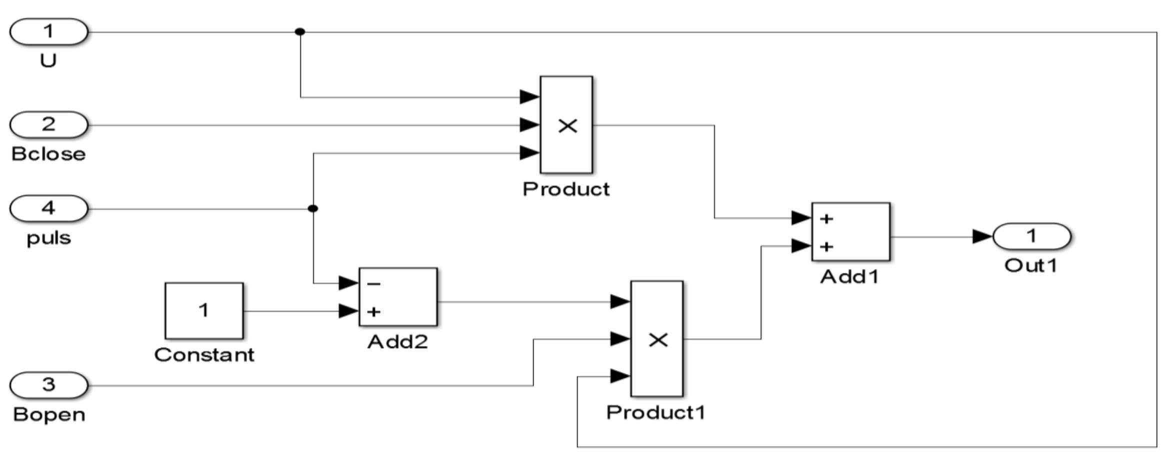

Figure 3-10 The B matrices of state spaces

Figure 3-10 is implementation of the B matrix for two states, where the input port 4 is the duty-cycle control signal to turn on and off switch. The pulse signal can be either zero or one to close and open respectively. Once the control signal is zero, port 3 is selected as the system output; the system outputs closed B matrix. Port 1 stands for the power source voltage that is a constant is.

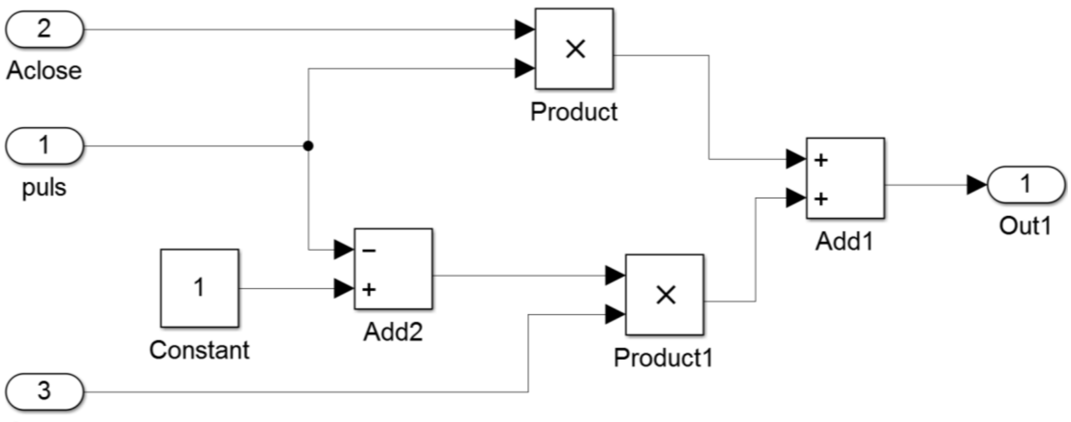

Figure 3-11 The A matrices of state spaces

The same strategy is used for matrix A model, it will also be controlled by the same pulse signal for matrix B case. By using a switch block that provides one or zero control signals, open and close systems can be altered easily. After building the subsystem models of the whole system, the matrix A Simulink is showed below.

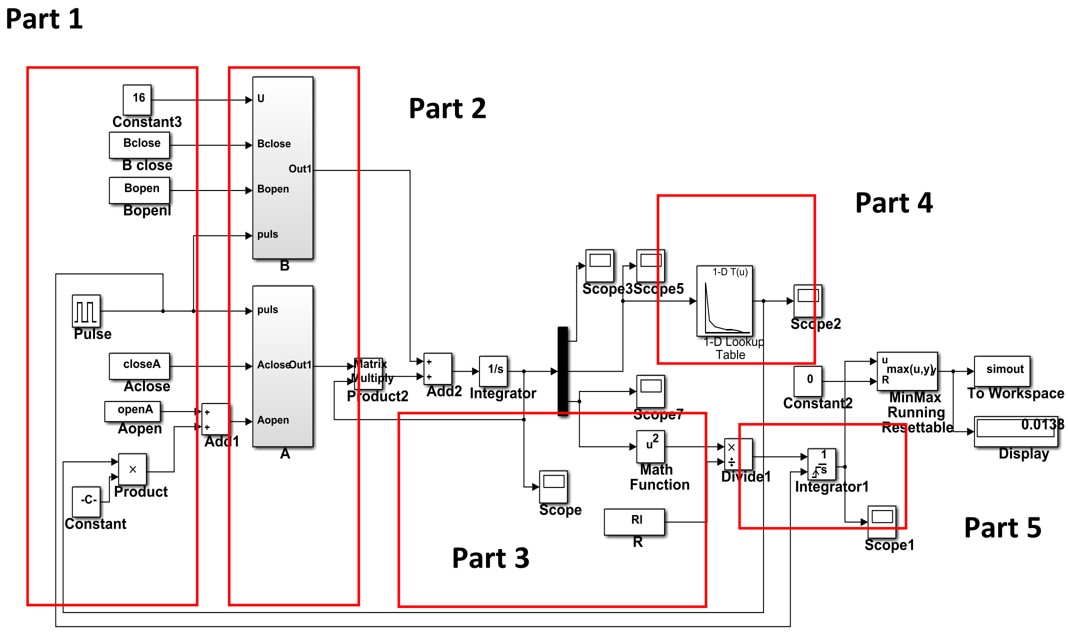

Figure 3-12 The state space model

Regarding the whole system model, it can be separated into five parts as shown in Fig 3-12. Part 1 is to provide the parameters of the whole system, where the matrix elements, input voltage and duty cycle are provide by a matlab script. With this method, modifying simulation parameters are easy and clear. Part 2 is the matrix selection part which is introduced in Figures 3-10 and 3-11. Part 3 is the integration for the whole state space model. Part 4 stands for the diode model. As the diode is a nonlinear component in the whole system, the better way is to use the V-I curve to model the diode resistance. In this function, current though the diode is a variable and the resistance is a dependent variable. For this part, the lookup table block is adopted. With the current of inductor inputting into the lookup table, the value of corresponding resistance is the output. Part 5 is the power output calculation model. Based on the definition of power output over a peroid, this model provides accumulated the work and reset it in a period. With this function, the power outputs generated during every period can be calculated.

3.1.3. Average Technique Simulation model

Average Technique was introduce in Chapter 2. For verifying the simulation performance of the developed model, a Simulink model is also developed as shown in Figure 3-13. The state-space model can be obtained by substituting (3.28) and (3.33) into (2.5).

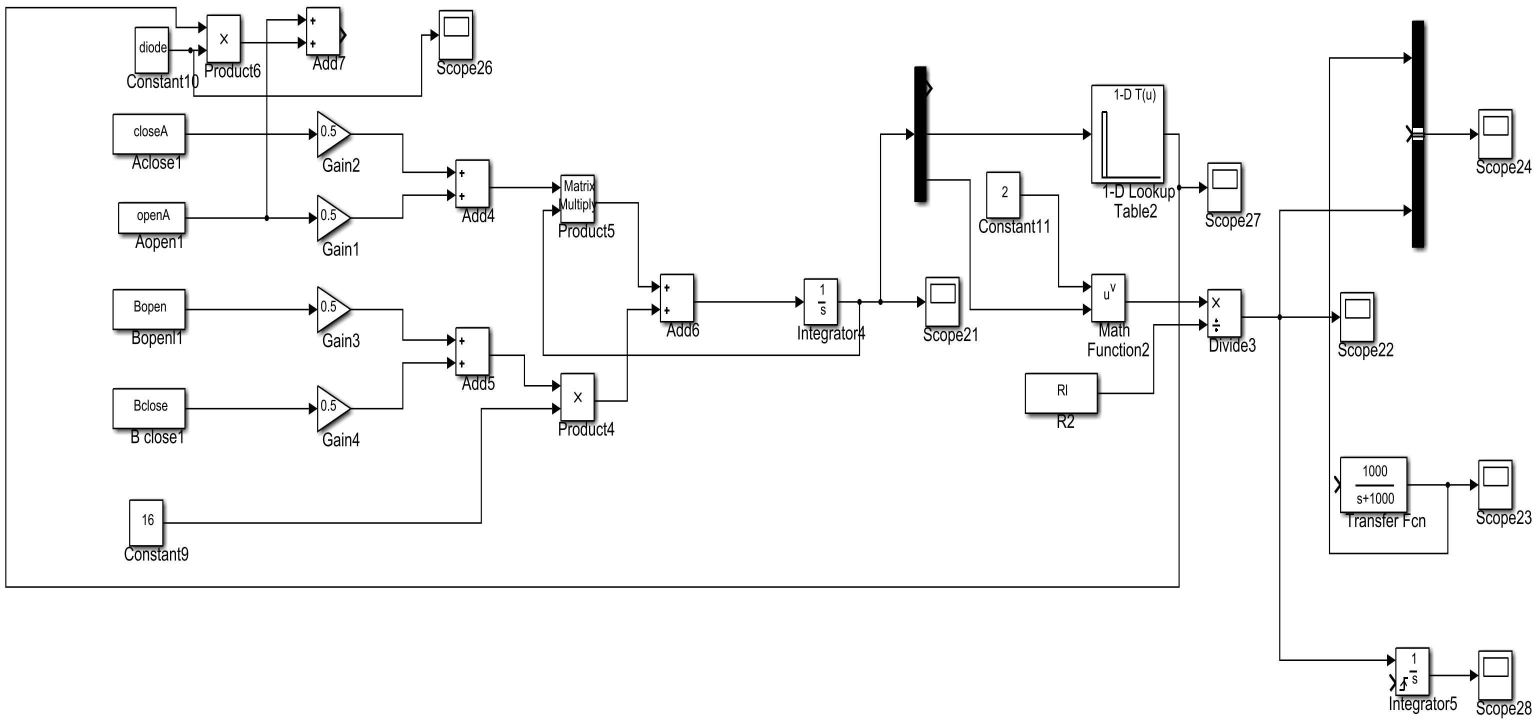

Figure 3-13 Average technique simulation model

3.2 Simulation with Simscape

After deriving the analytic solutions of primarily improved circuit and final optimized circuit buck converter, simulation based upon the matlab/Simulink Simscape toolbox is conducted. Simscape toolbox provides a simulation environment of modeling physic systems as such as hydraulic, mechanic and electric systems. According to the introduction from Matlab, Simscape toolbox can be used to design control system and study system-level performance. Since Simscape supports c-code generation, the designed model can be deployed in different environments.

3.2.1 Simulation Model of Primarily Improved Circuit

In this section, the process and strategy of building simulation model for the primarily improved circuit model is discussed. Within the Simscape toolbox, the circuit can be implement according to the figure 1-7. The capacitors, resistors, constant voltage resource and switch are base function blocks in Simcape. In order to simulate the model, a numerical solver needed to be configured in the Simscape toolbox. Regarding the circuit, a electrical reference is also need to the circuit. Square pulse block is used to control the switch. In order to connect the blocks from basic toolbox with the simscape blocks, two transfer blocks are required which are also from the utility content of simscape toolbox. The sensor block in the Simscape is used to output the measured signal

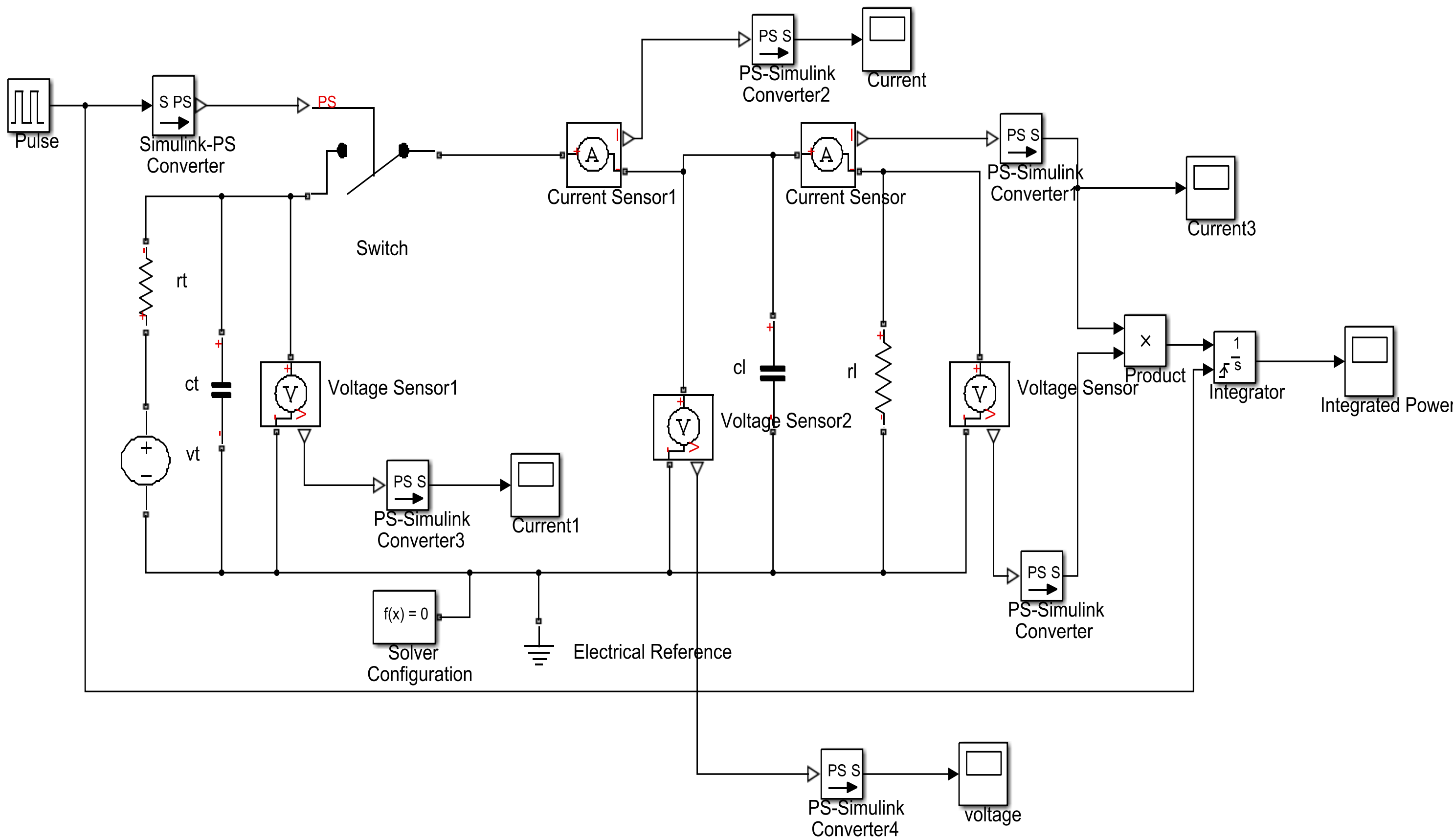

Figure 3-14 the Simulation model of primarily improved circuit

Regarding the model simulation parameters, the fixed-step was selected as the solver type since it was challenge to make variable-step simulation. Adopting variable-step solver led to high simulation error and cannot generate stable power output. Also, the variable-step solver was very slow compared to the fixed-step solver. In this case, the fixed-step type solver is a good option. The order of solver was set to 14 in simulations. It uses a combination of Newton's method and extrapolation from current value to compute the model's state at the next time step as introduced in Matlab. Both the accuracy and the efficiency satisfy the requirement of this model. Since the period of the pulse which control the switch is 0.0001s, the simulation time is set as 0.01s that covers 100 cycles. It is long enough for simulation to approach steady state. The time step size was set as 0.000001s. Which calculates 100 times in one period. The accuracy and speed of simulating are both assured by this method. In order to improve the accuracy, the extrapolation was selected as 4. The other parameters are also determined by try and error. The parameters are shown in figure 3-15.

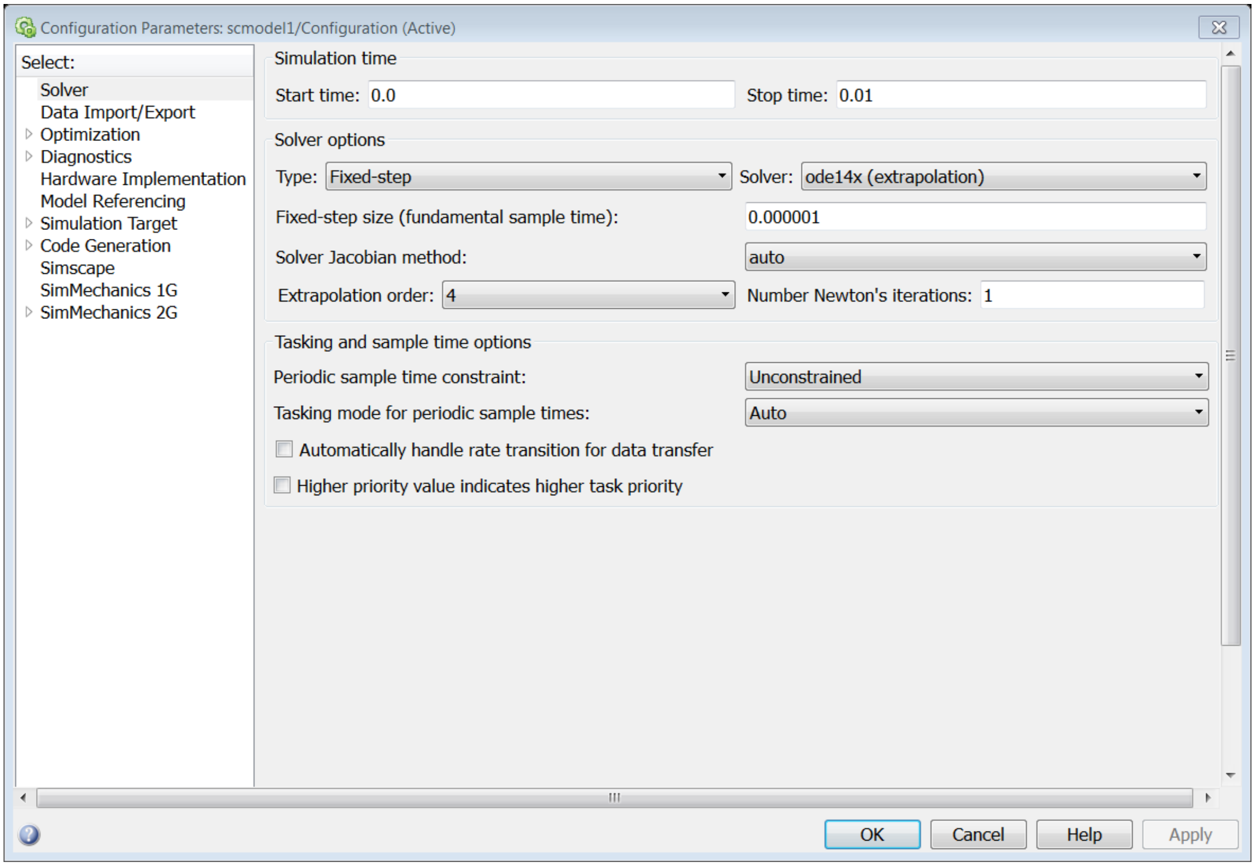

Figure 3-15 Simulation configuration parameters

The method of collecting data is introduced in this paragraph. The main data wanted is the power output over one period and the current ripple on the lead resistance and switch. The high current ripple. Regarding the power output, it has already discussed in the section that describes the state space. Part of the method is continued using here in the simscape simulation model. According to the definition of power generated by circuit, voltage over a component multiplies its current is the power output. Applying this principle on load resistor R_l, the power output signal can be generated by multiplying the voltage and current on it. In order to figure out the amount of work done by the load resistor, the power output has to be accumulated over the peroid. For this reason, the integral block is used here. The type of integral is set as rising type which makes sure the work can be reset each period. The signal of reset time comes from the pulse block as it is the period for the whole system. To record the data, a variable is set in the scope for the power output signal. This variable is recorded into the workspace. The same recording method can also be applied to the current ripple data collection. By the definition of ripple, the difference of maximum current through the switch and minimum current are calculated by programed script.

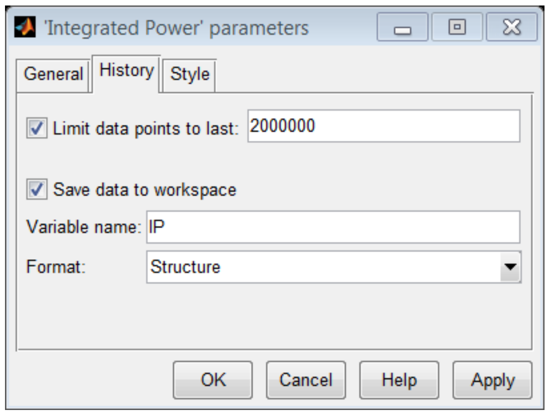

Figure 3-16 Data collection setting in Scope

3.22 Simulation Model of Buck Converter

Development of the final optimized circuit model in Simscape tool box is quite same as the process for the primarily improved model. The main different is the structure of the circuit. Comparing with the primary one, an inductor and a diode added in to the circuit. The diode is required to be configured. The default resistance of diode block 0.3 Ω is much large than expected value.

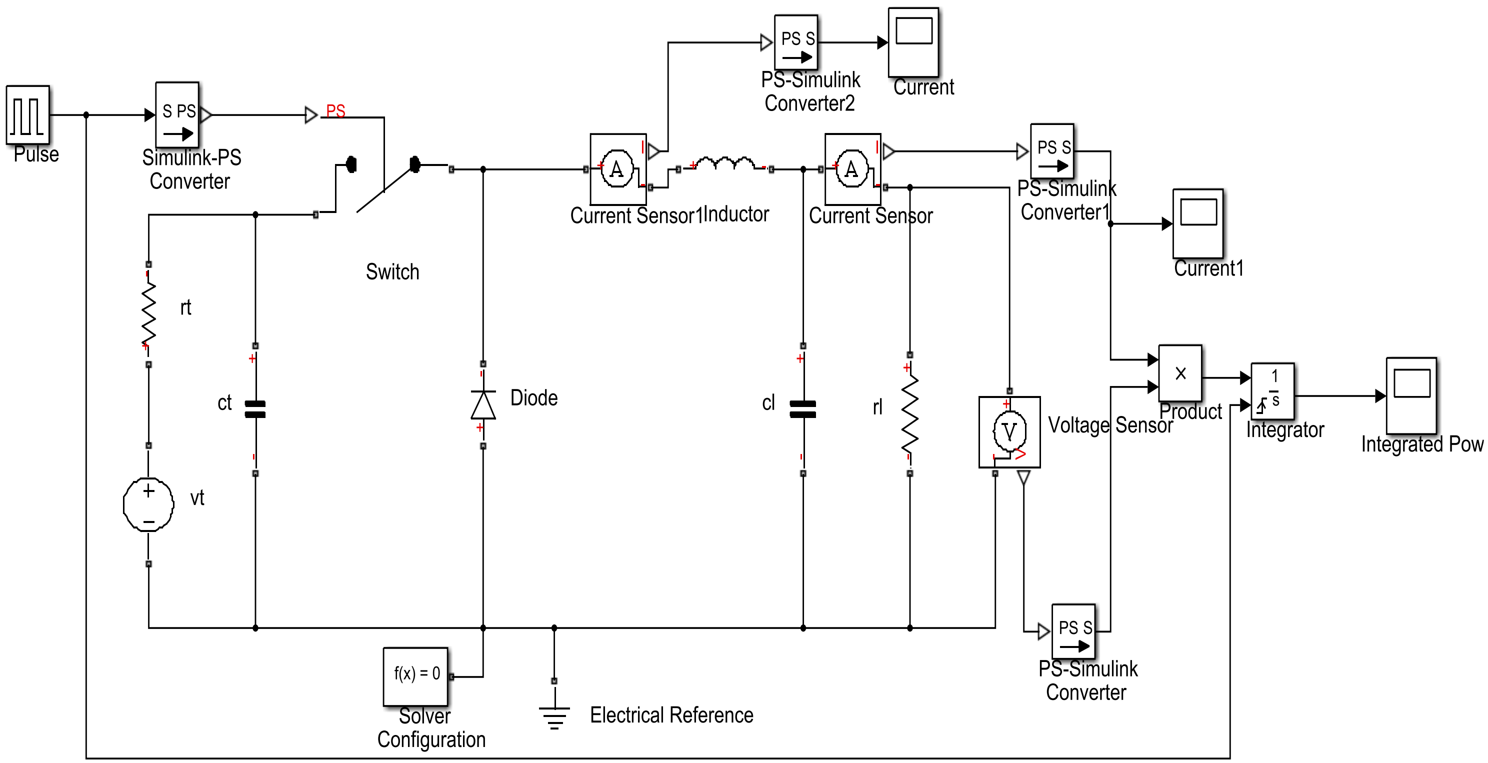

Figure 3-17 Buck converter simulation model

3.3 Results Comparing

To assure the accuracy of model work, running different models, developed using different approaches, and comparing the simulation results are quite necessary. In this section, the goal of conduct simulations using different models is to validate the accuracy of the models and decide the model to be used. The first couple of models to be compared are the primarily improved circuit model with its analytical model, and then followed by the buck converter models. The accuracy and efficiency of state space simulation model and Simscape simulation model are the target to be analyzed. The final comparing was focused on the performance of buck converter model and primarily improved circuit model. The power output and efficiency are to be compared in this section. In order to keep simulation results choose to the realistic experiment requirements, the electric source is set to 16 volt and the internal resistance is 0.5 Ω.

3.3.1 Comparing Primarily Improved Circuit Model and Analytical Solution

The power output of the circuit is the key variable to be compared between these two models. The selected simulation parameters are listed in the following table. The parameters were selected randomly. In order to make the comparing result more general, several sets of parameters were used.

Table 3-2 Parameters of improved circuit (3)

C_t (volt)	C_l (volt)	R_l (Ω)	Duty Cycle (%)
300e-6	40e-6	0.2	1 to 100

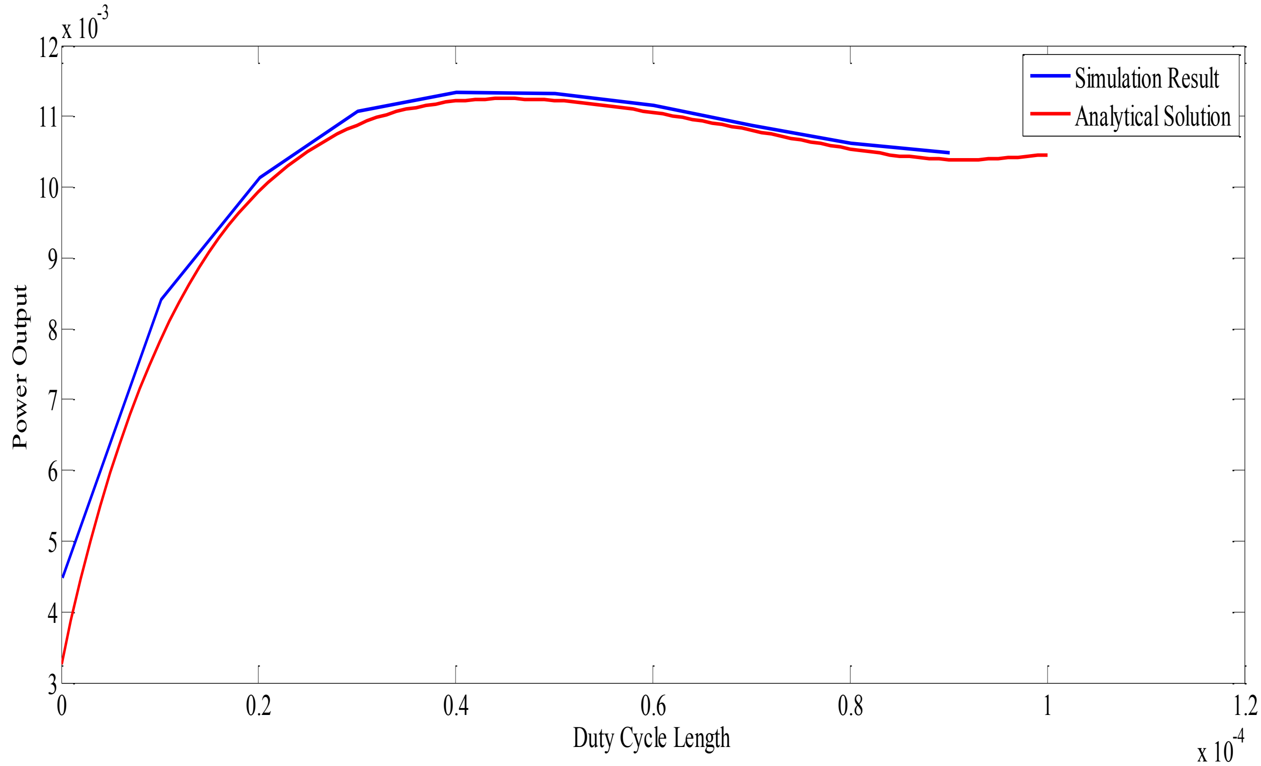

Figure 3-18 Simulation and analytical results

In Figure 3-18, the blue curve stands for the relationship between power output and the duty cycle time of the analytical solution; and the red curve is from the Simscape simulation model. From the figure, it is obviously two curves almost matches with a slightly gap. The gap could be caused by the integral solver. As the simulation in Matlab is realized by solving the continuous differential equations step-by-step. However the difference between these two methods is fairly smaller. The simulation model is accurate enough for study. As the beginning of the simulation, there is a considerate value of power output with the duty cycle approaches zero. This could be duel to the voltage pulsation between C_t and C_l at switch. Which causes the energy stored in Capacitor C_t transfers to C_l instantly. According to the trend of the curve, with the increasing of duty cycle, the power output increases. The main point to be emphasized is that at certain duty cycle, the power output is larger than the power output of the circuit without control. The Power output of original circuit supposed to be 0.01041 W. The max power output of the primarily improved circuit is almost 0.0113W. This indicate that the output power could be increased by for controlling the duty cycle.

3.3.2 Comparing of Buck Converter State Space Model and Simscape Model

This section, is to verify the accuracy and performance of the Simscape simulation model. The method verifying to is also compared with the target analytical model. The state space analytical model of the target buck converter was also implemented into Simulink with basic mathematic tool box. There are advantages for the comparing model since the two simulation models can be run simultaneously, which makes it easy to compare simulation results. The Combination model are shown in figure 3-19.

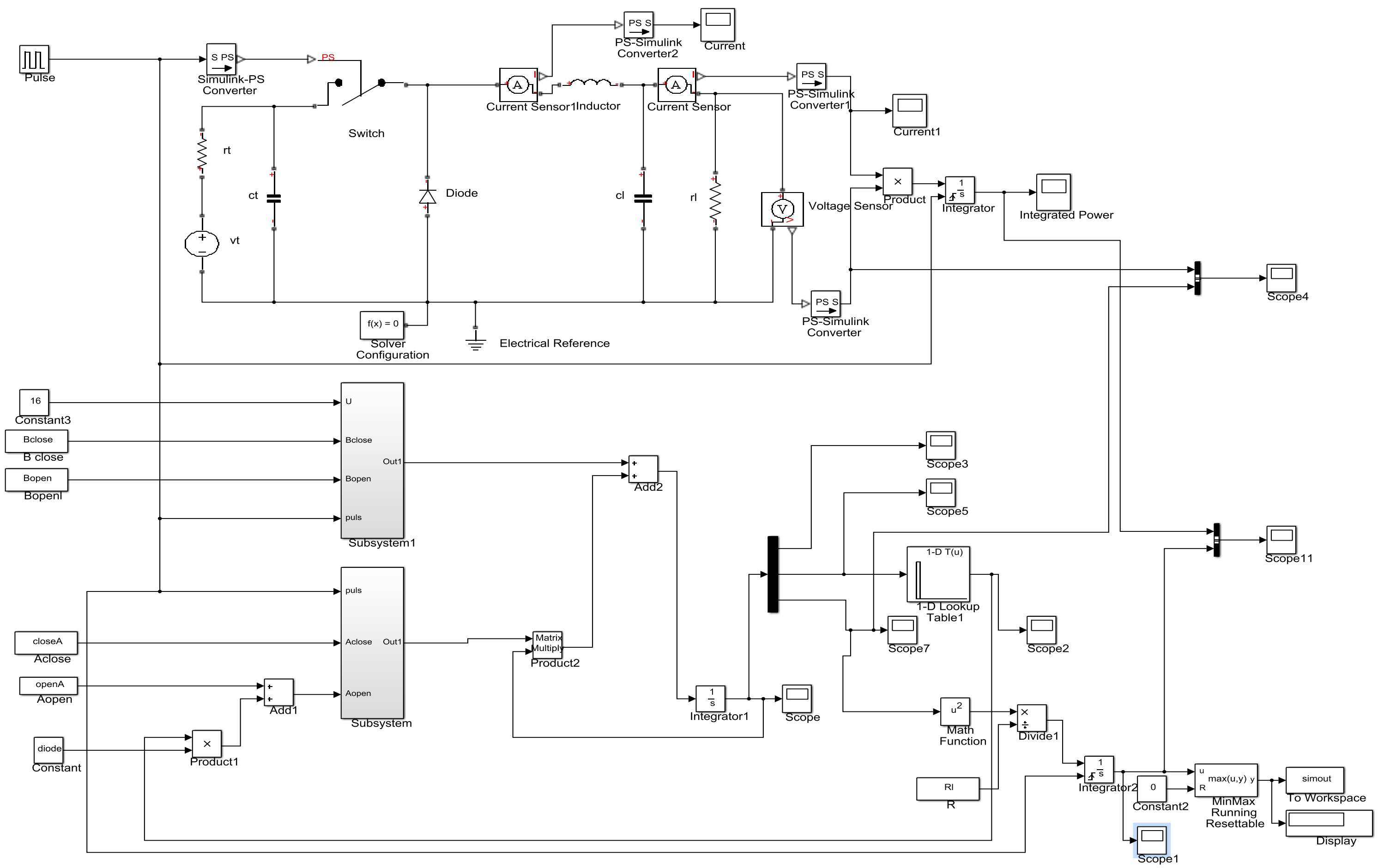

Figure 3-19 Combination model of buck converter and state space

Two models shares the same pulse to control the switch for the whole system. The benefit of sharing the same pulse is that two system models can run synchronously. Another advantage is that it is easy to compare the output signals with one scope. The parameters for configuring the circuit model are selected by try-and-error based on realistic experiment data.

Table 3-3 Parameters of buck converter (1)

C_t (F)	C_l (F)	L (H)	R_l (Ω)	Duty Cycle (%)
250e-6	30e-6	30e-6	0.3	80

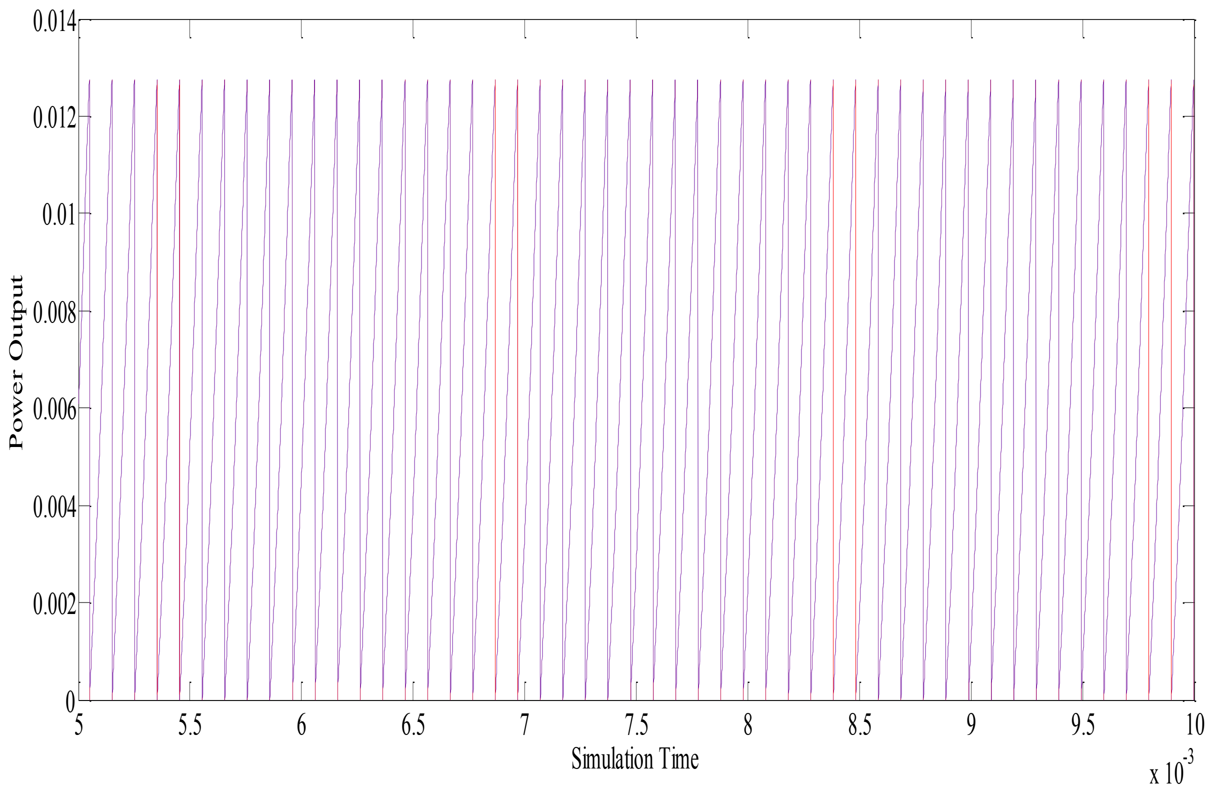

Figure 3-20 Power output of buck converter (1)

The curve in Figure 3-20 shows the relationship between power output and simulation time, where two curves are from different models and matches very well. The accuracy of the Simscape simulation model is verified by the state space analytical solution model. According to the parameters selected for this simulation model, the power output of the corresponding original circuit is around 0.012w. With the simulation of 80% duty cycle, the power output approaches 0.0125 w. It can be predicted that with further, power output could be future improved.

3.3.3. Comparing of Primarily Improved Model and Buck Converter Model

The difference between two circuit models is that there are an inductor and diode added to buck converter model comparing with the primarily improve model. The inductor reduces the current ripple between the two capacitors. The diode is a passivity component which supposed to have not much energy consuming. Decreasing the inductance reduces the difference between two circuit systems. The parameters are selected as following.

Table 3-3 Parameters of buck converter (2)

C_t (F)	C_l (F)	L (H)	R_l (Ω)	Duty Cycle (%)
250e-6	30e-6	10e-6	0.3	1 to 90

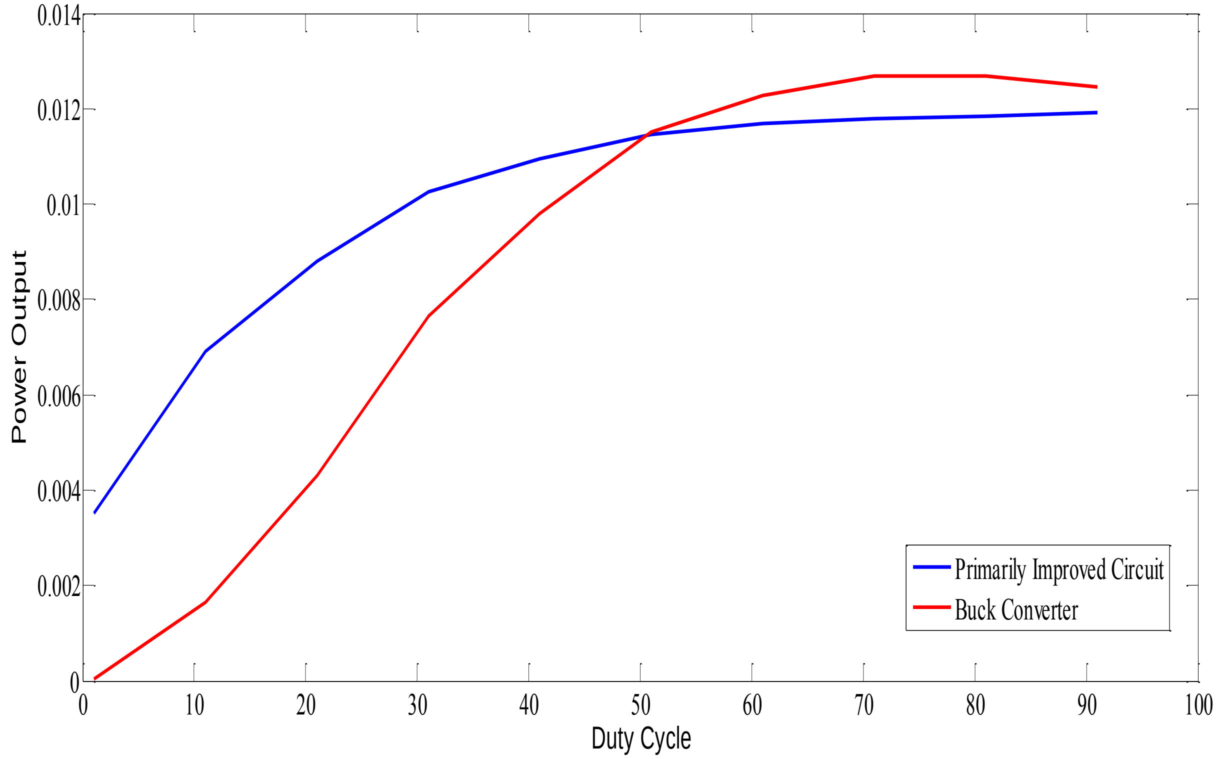

Figure 3-21 Relationship of power output and duty cycle

From the figure above, the buck converter is able to generate higher energy than the primarily improved circuit the duty cycles is higher than 50 percent. However when the duty cycles is lower than 50 percent, the primarily improved circuit model can generate more energy than the buck converter model. The power output of the buck converter approaches zero as duty cycle. Note that the simulation of the primarily improved circuit is not accurate when the duty cycle is low. The reason is that the primarily improved model transfers energy from capacitor C_t to C_l unrealistically since the voltages of C_t and C_l have to be equal at an instant once the switch is closed. This action could lead to a significantly high current between C_t and C_l. When the duty cycle is low, the capacitor C_t is charged longer than the case with high duty cycle. As a result, the capacitor C_t also stores more energy. And this energy will be transferred to C_l in an instant for primarily improved circuit. However in the buck converter, due to the effect of inductor, the current cannot change rapidly. So the primarily improved circuit has advantage in the efficiency of power output under low duty cycle. However the extremely high current generated at the instant of the closing switch is not realistic and cannot be realized. It could make the switch component be damaged due to over current. Considering the high duty cycle cases, the buck converter circuit model can deliver even more energy as the inductor can also stores certain energy.

3.4. Conclusion

In this chapter, analytical simulation models of primarily improved circuit and final optimized circuit are developed. Differential equations and state space method are developed to verify the performance and accuracy of the Simscape simulation models. Through simulation study, it was found that the final optimized circuit significant advantage over the primarily improved circuit. As a result, the buck converter is selected as the finalized circuit due to the fact that it is feasible for implementation. By observing the result of the simulation model, it can be concluded that it is necessary to control the buck converter circuit to maximize the power output. These conclusions drawn based upon the circuit before the parameters are optimized. The parameter optimization will be addressed in the next chapter.

Chapter 4 Simulation Study and Configuration

The buck converter designed in the last chapter contains three by components which needs to be configured. They are inductor L, capacitor C_t close to electric source and capacitor C_l close to the load resistance. In order to study the characteristic of the target buck converter and design a controller for it, these three parameters needs to be optimized.

The goal of optimizing the circuit parameters is to assure the good circuit performance under various operational condition. The two performance target considered are the power output and the current ripple. Increasing the power output of this circuit under different load resistance is the motivation of this research. The duty cycle control will be used to deliver the maximum power. On the other hand, reducing ripple is also necessary in order to deliver high quality DC power. The circuit parameters can also impact current ripples. By analyzing the circuit, the switcher is a high duty-cycle component used as the control actuator of the system. When the switch is closed, high current ripples occurs duel to voltage difference between two capacitors. The energy transferred through the switch is considerably high. For this reason, study is focused on the current though the switcher.

The goal of selecting the circuit parameters is to maximize high power output with the help of duty cycle control for a reasonable ripple level. Making a good trade-off of power output and current ripple by selecting a set of circuit parameters is the goal of this chapter.

4.1. Strategy of Configuring Circuit

The performances of the circuit mentioned at the beginning of Chapter 4 is the standard for selecting circuit parameters. With the controller, the power output can be approach maximized. The optimized a circuit parameters with closed-loop are to be found numerical simulations results.

The first step is to determine the range and increment of possible parameters. The parameters contain duty cycle, load resistance, capacitor values and inductor value. The duty cycle and load resistance are parameters depending on working conditions and control range. The other three parameters are to be determined in this chapter. The controlled duty cycles will be used to maximize the power output. With the determined the range and increment of the duty cycle, a vector can be selected for the possible duty cycles. For example, if the range of feasible duty cycle is between 1 percent and 100 percent, the duty cycles vector can be selected as T=[10 20 30 40 50 60 70 80 90 100]. Where the 10 percent is the increment of the duty cycle. The optimized duty cycle lead to maximum power output is probably not concluded in this vector. However the optimal cycle. With smaller increment of duty cycle, the optimal duty cycle could be approached closely. The range of the duty cycle is determined to be from 1 per cent to 100 per cent at first. The analysis that the circuit will not deliver satisfied power with small duty cycles. In order to fine a set of optimal parameters for the circuit, the load resistance variation is also needed to be considered. The same approach to duty cycle can be applied for load resistance validation. Assuming that the load resistance ranges from 0.1 Ω to 1Ω, the vector of varying load resistance can be expressed as R_l=[0.1 0.2 0.3 0.4 0.5 0.6 0.7 0.8 0.9 1]. The Range of other three parameters can be acquired in the similar way.

The second step is to collect the simulation data of power output and current ripple with running simulation model. By programming matlab script, the simulation model can be controlled to run under different parameters and the associated simulation data can be also collected. The collected data can be arrange to form matrixes and saved in matlab work space.

The third step is to process data and compare results. The process of data is introduced in Figure 4-1. The process is to study the effect of control using a matlab script. The optimal control can be found for the maximum power output. The next step is to calculate the summation of the maximum power output values the set of parameters. The sum of power output with different load resistance for a given set of parameters C_t, C_l and L can be found. With the corresponding parameters of the power output, the associated ripple can be easily and obtained. After analyzing data, the results can be found. Usually, the curves and surfaces of the power output, ripple as function of the varying parameters can be used to find the optimal parameters.

`

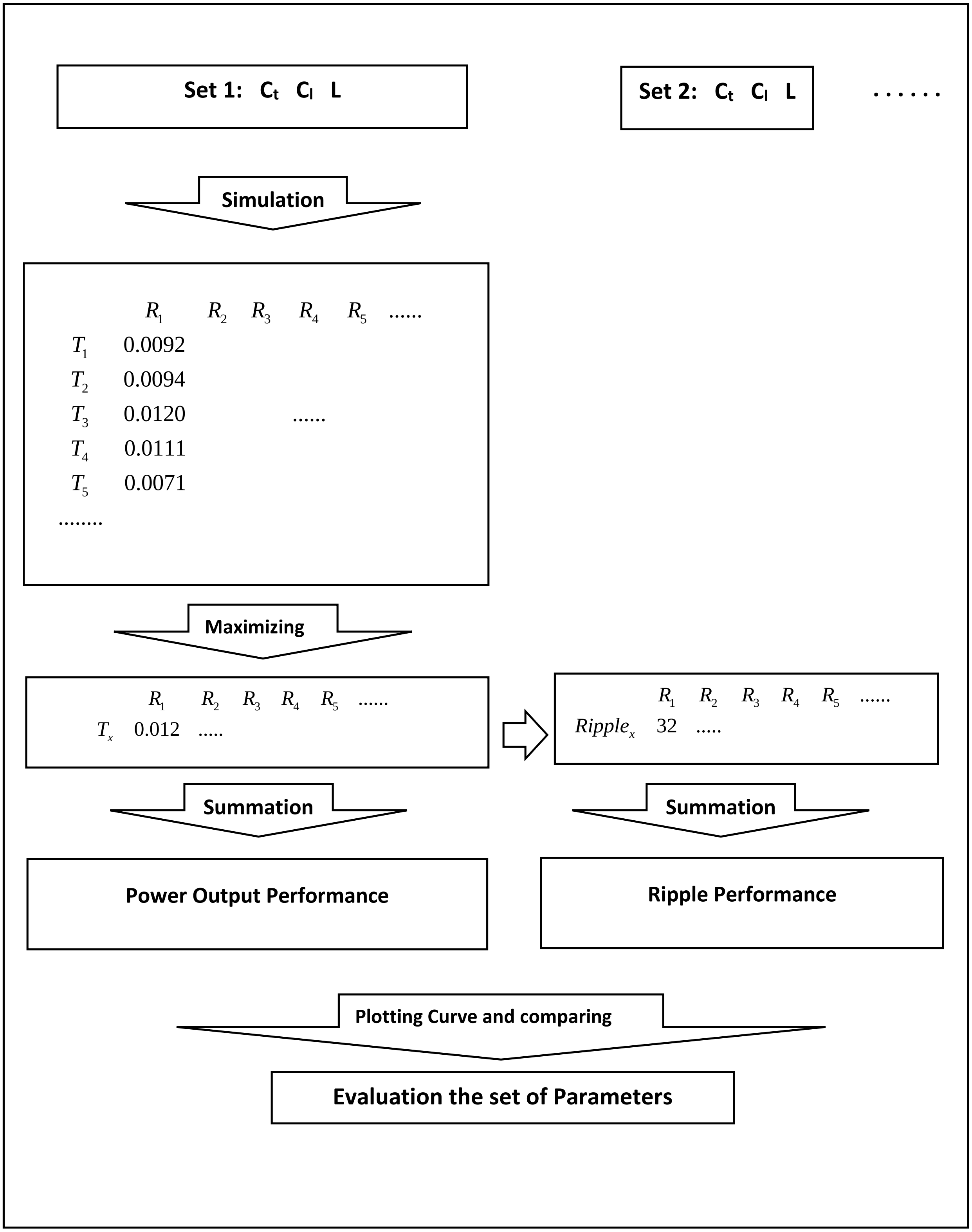

Figure 4-1 Flow chart of data processing

In summary, a set of matlab scripts are programed for simulating the circuit system with given contoal parameter. With them the expected power output and the corresponding ripples can be obtained Simscape buck converter.

4.2. Load Resistance

For finding the optimal circuit parameters, the load resistor is one of the components needed to be studied. The load resistor varies with connected electric device. Because the research is focused on simulation, the load resistance is assumed to be constant.

As the internal resistance thermal electric generator is defined as a constant 0.5Ω, the range of load resistance need to be studied will be in the neighborhood of internal resistance. Recall that in Chapter 1, it shows that the power output can be increased by switch control in Figure 1-9. In Figure 1-9, the power output of the controlled circuit is higher than the original circuit when the load resistance is smaller than 0.3Ω. Therefore, it is important to control the switch when the load resistance changes. Simulation study was conducted to find the optimal duty cycle. The parameters used for simulation is listed as following.

Table 4-1 Buck converter parameters (3)

C_t (F)	C_l (F)	L(H)	R_l(Ω)	Duty Cycle (%)
350e-6	20e-6	20e-6	0.1:0.1:1.5	10:10:100

After running this model and processing the simulate data, the relationship between maximum power output and load resistance is obtained in Figure 4-2. Comparing it with the curve of original circuit, it can be seen that the power output is enhanced when the load resistance is smaller than 0.5Ω.

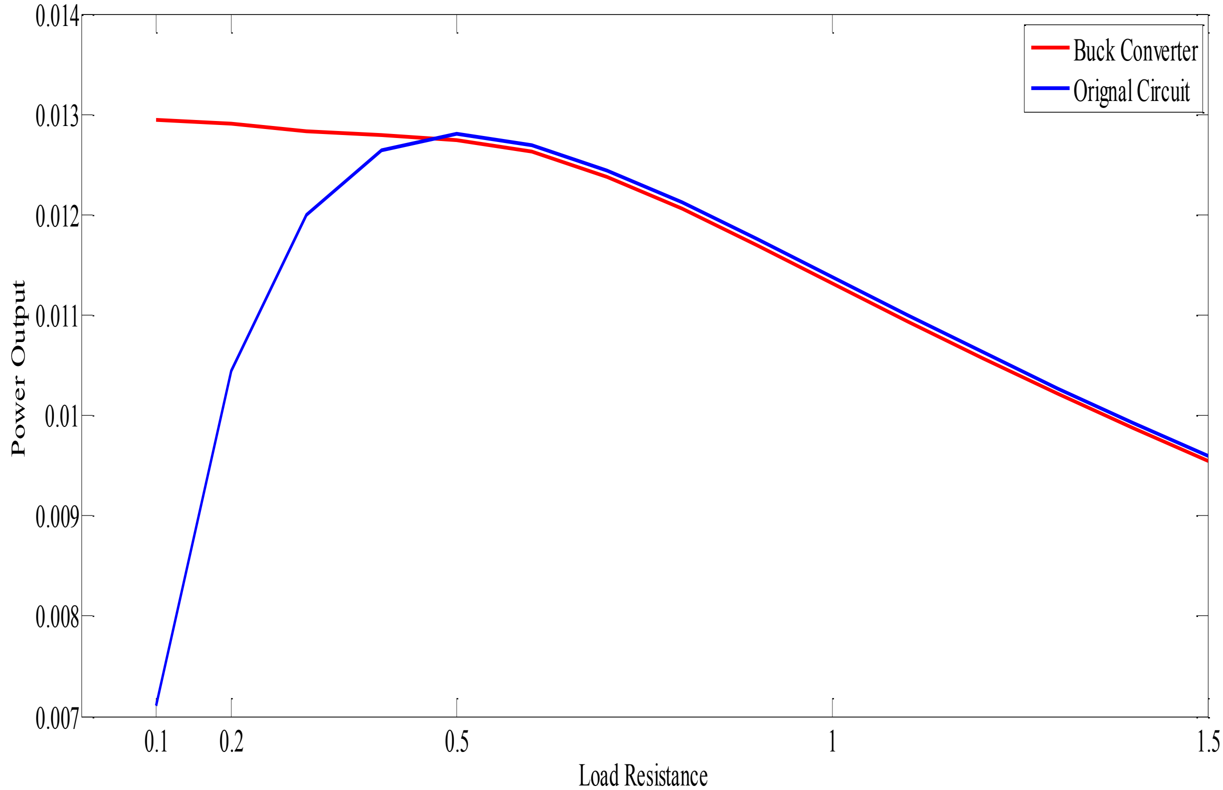

Figure 4-2 Relationship of power output and load resistance

From the figure, it is clear that when the load resistance is smaller than the internal resistance the power output can be increased through duty cycle control, and when point of the load resistance is greater than the internal resistance the power output cannot be improved. After running the Simulink mode with other parameters, the conclusion remains the same.

4.3. General Simulation

The central goal of parameter optimization is to find a set of parameters that yield reasonable current ripple and power output. The first step is to find out how these parameters affect the circuit performance. In this section, some general simulations are conducted to figure out the relationship between the circuit performance and the parameters. The internal resistance and the power source are fixed at 0.5Ω and 16 V, respectively.

If the parameters are not mentioned specially, the values defined in chapter 3 are used. The range of the following parameters are selected according to the design limits and implemetation consideration.

Table 4-2 General simulation parameters

C_t (μF)	C_l (μF)	L(μH)	R_t (Ω)	Duty Cycle (%)
50:100:450	8:30:158	8:30:158	0.1:0.1:0.6	10:10:95

The range of these parameters covered the possible combination for the target buck converter. The results are shown below.

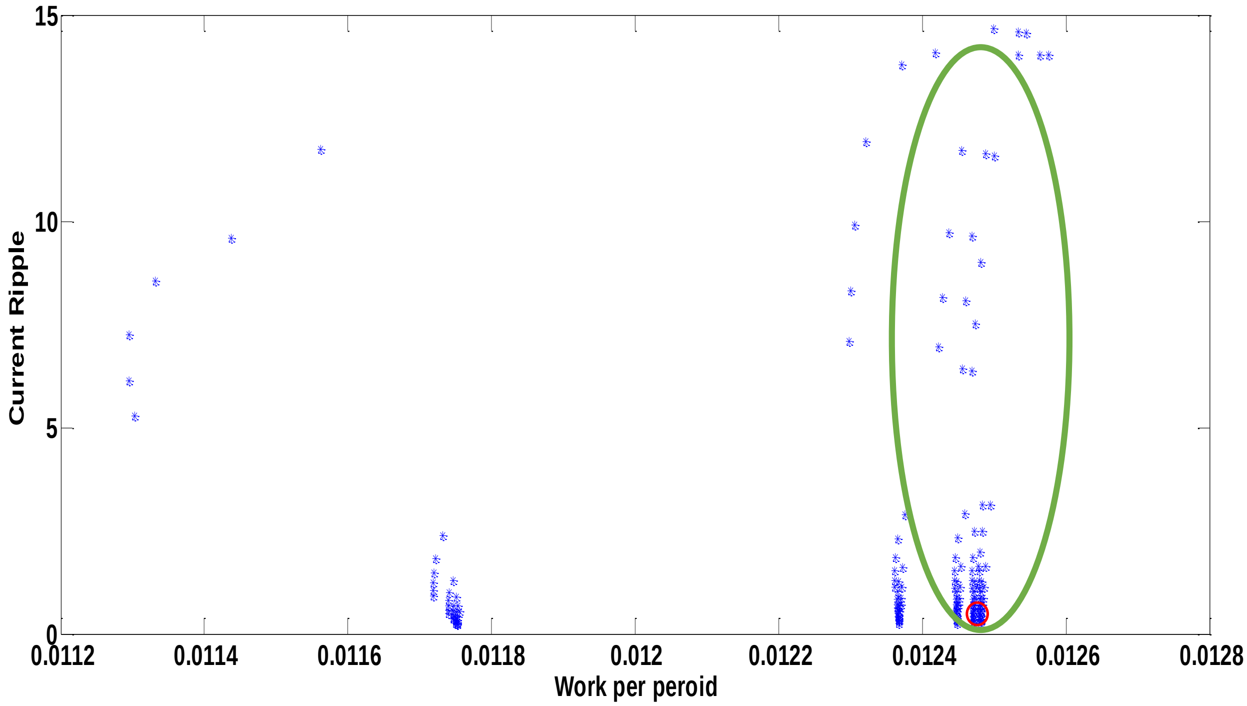

Figure 4-3 Performance of circuits with different parameter sets

The Figure 4-3 shows the performance (ripple and power output) of circuit with different sets of parameters. Each point in the figure stands for a pair of power output and current ripple with the unique set of parameters. It is obvious that the asterisks close to the lower right corner in the coordinates represents for the most desirable performance and hence, the parameter sets. In this case the current ripple is low, and the power output is high. In this figure, the asterisks inside the red circle are to be selected. There might be a tradeoff between the two performance indexes: current ripple and power output. The selection with emphasis the balance of power output and current ripple to be discussed later when the detail simulations are available. There is a certain tradeoff between the current ripple and peak power output shown in the green circle.

There are three parameters to be selected and we are going to study their effects to system performance individually.

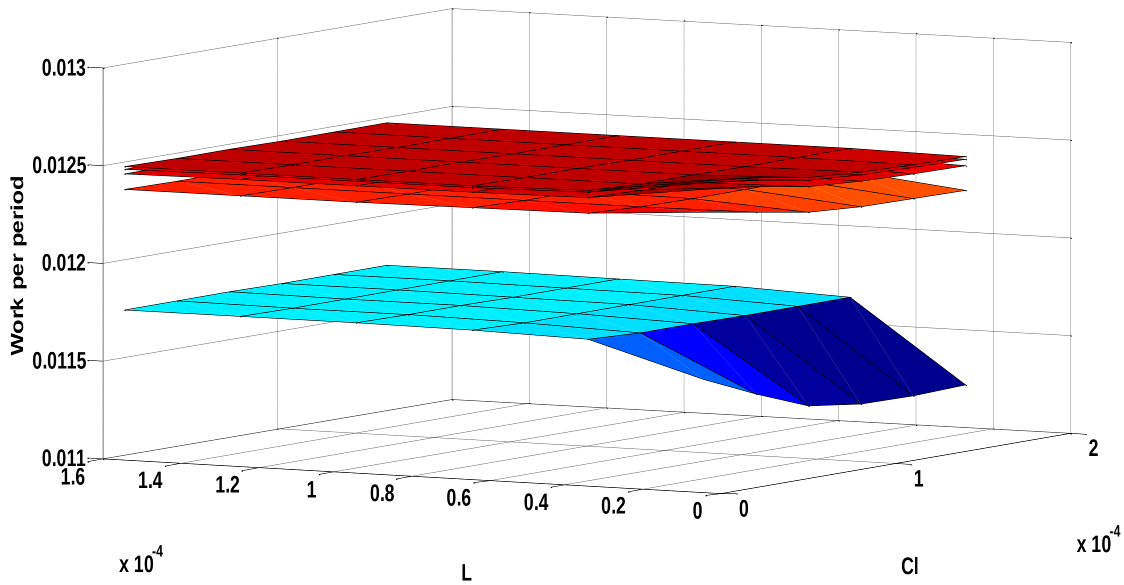

Figure 4-4 Power output performance

In Figure 4-4, it can be seen that there are six surfaces in the figure. Using the matlab coded script in appendix, the six surface stands for six values of capacitor C_t. On each surface, the maximum power output is varying depending on the variable C_l and L, where the target parameter going to be discussed is C_t. Form the figure, the conclusion can be made that with the C_t increasing, and the power output of the circuit increases. And the rate of increment reduces as the C_t increases. With the capacitance of C_t increases the capability of C_t to store energy improves also. This implies that the power delivered from C_t to C_l is also increasing.

However, the capability of power delivering from C_t to C_l is also depends on other factors, too. Once the capacitance become too large, the power output cannot be further enhanced as shown in Figure 4-4.

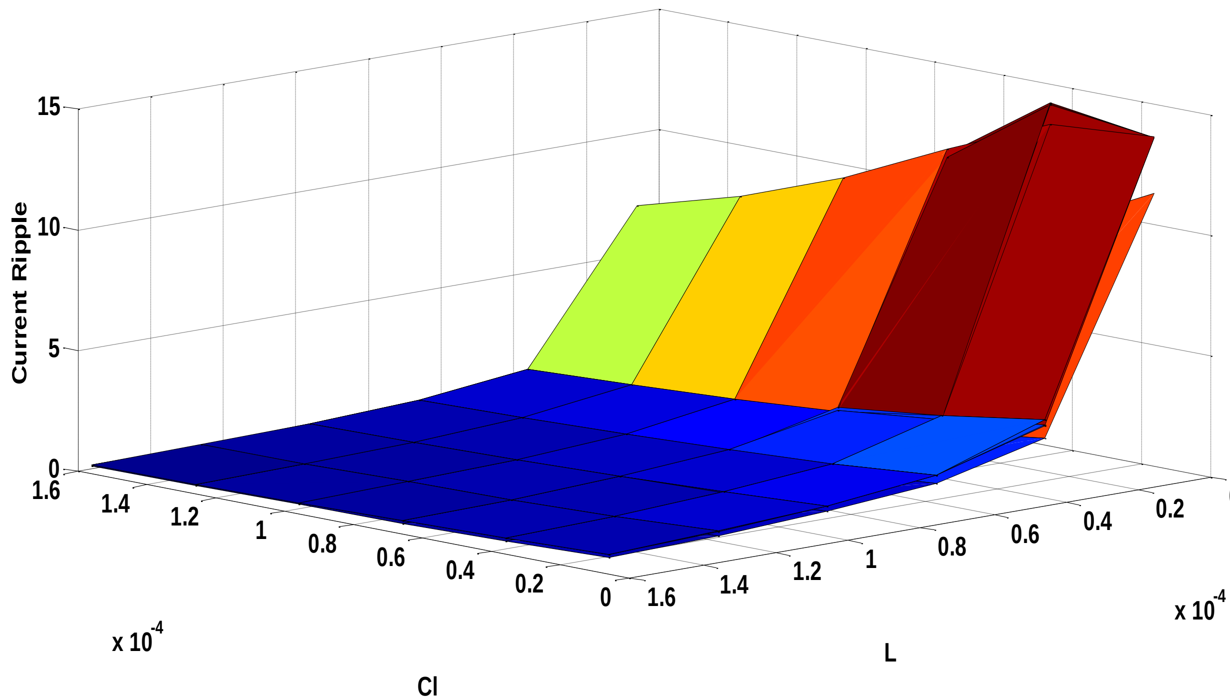

Figure 4-5 Load resistance current ripple performance

The Figure 4-5 presents the relationship between current ripple and Capacitor C_l and inductor L. Different surfaces stand for different C_t value. As it is shown in Figure 4-5, with the C_t increasing, the current ripple increases. The increment rate of current ripple decreases. Regarding C_t, a tradeoff needs to be made that the ripple and current has the same trend with the increment of C_t. The possible value is around 200 µF.

After studying the trends regarding C_t, we are going to take a look at the relationship between the performance and parameters C_l, L as well. For each surface in Figure 4-4 and figure 4-5, the front views show the performance variation with the L. In Figure 4-4, the power output changes significantly with the L at the beginning. After L approaches to 80 µH, the output power remains unchanged, so either does the C_l cannot impact. In Figure 4-5, the current drops very quickly as L increases. After the L approaches 80 µH, the current hardly changes also. It is clearly that the inductor L will not change the system performance if it is greater than 80 μH. As shown in C_l direction, the power output is decreases with the C_l increases. When C_t is larger than 100 μF, the impact of C_t is minimum. It can be concluded that the ripple increases as C_l goes up. Therefore, the value of C_l small to be less than 100 μF.

4.4. Detail Simulation

After conducting the case simulations, the specific range of C_l and L are determined. This section conducts further simulations to determine C_l and L. The parameters are exists in Table 4-3.

Table 4-3 Detail simulation parameters

C_t (μF)	C_l (μF)	L(μH)	R_t (Ω)	Duty Cycle (%)
400	6:3:30	6:3:30	0.1:0.1:0.6	10:10:95

The following figures shows the performance of the circuit for all selected parameter combinations.

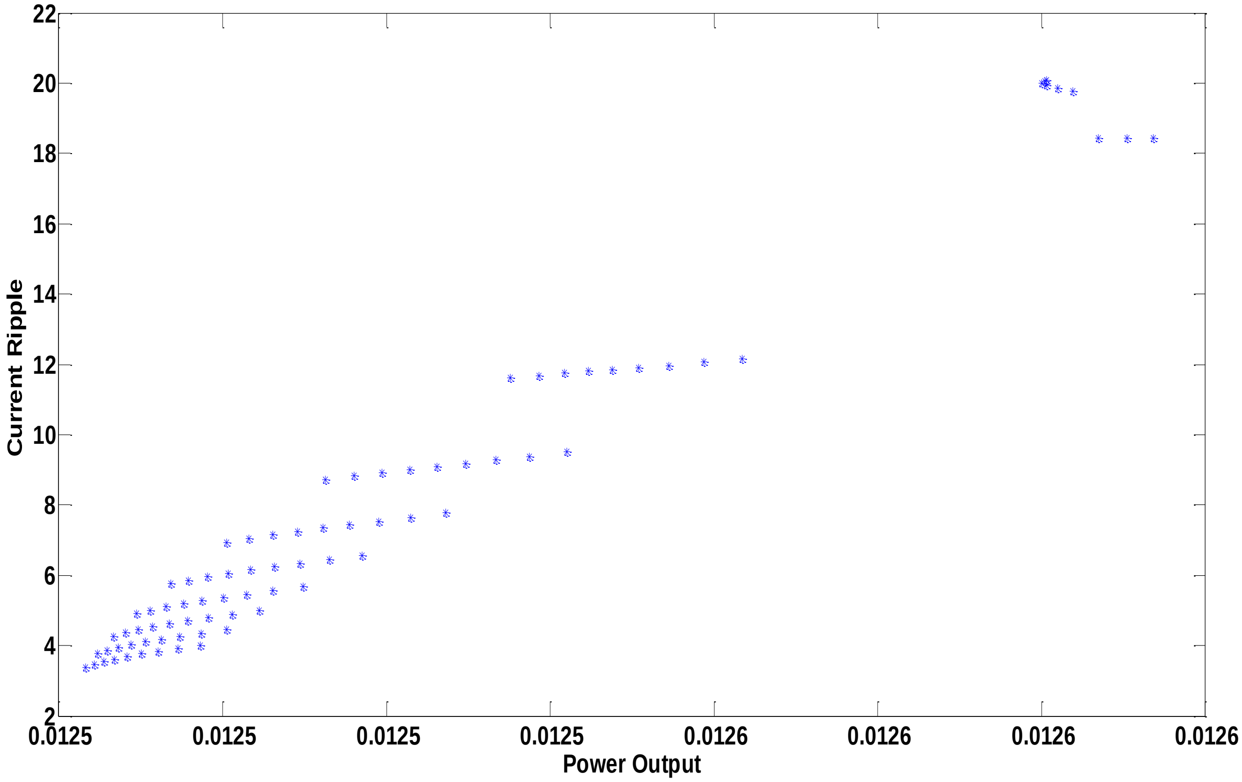

Figure 4-6 Performance of circuits with different parameter sets

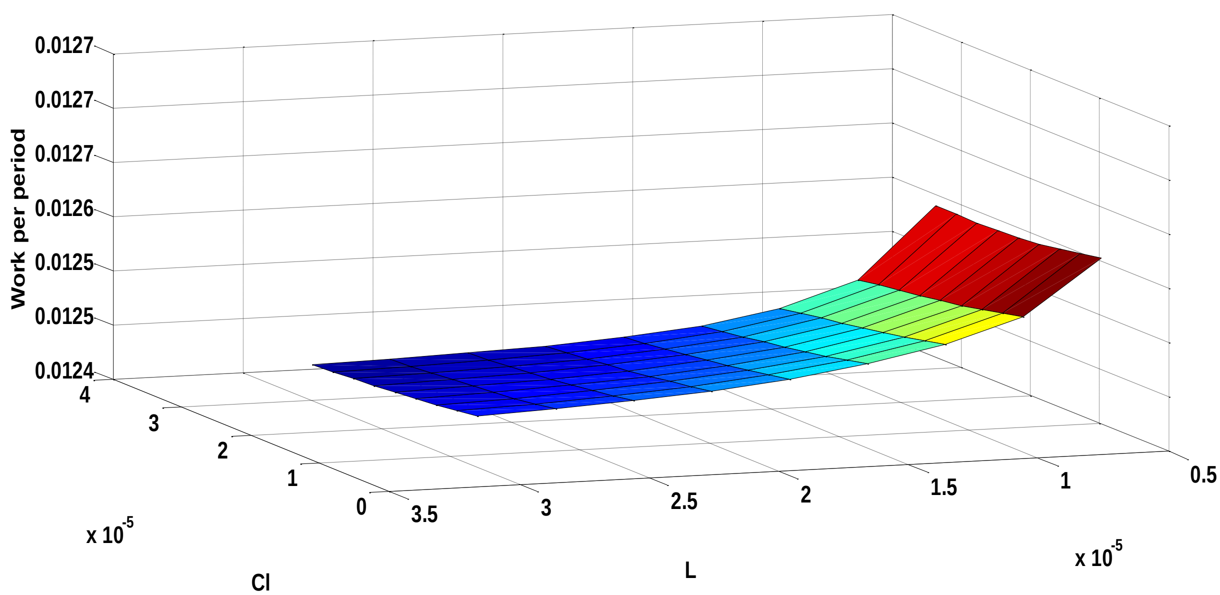

Figure 4-7 Power output performance

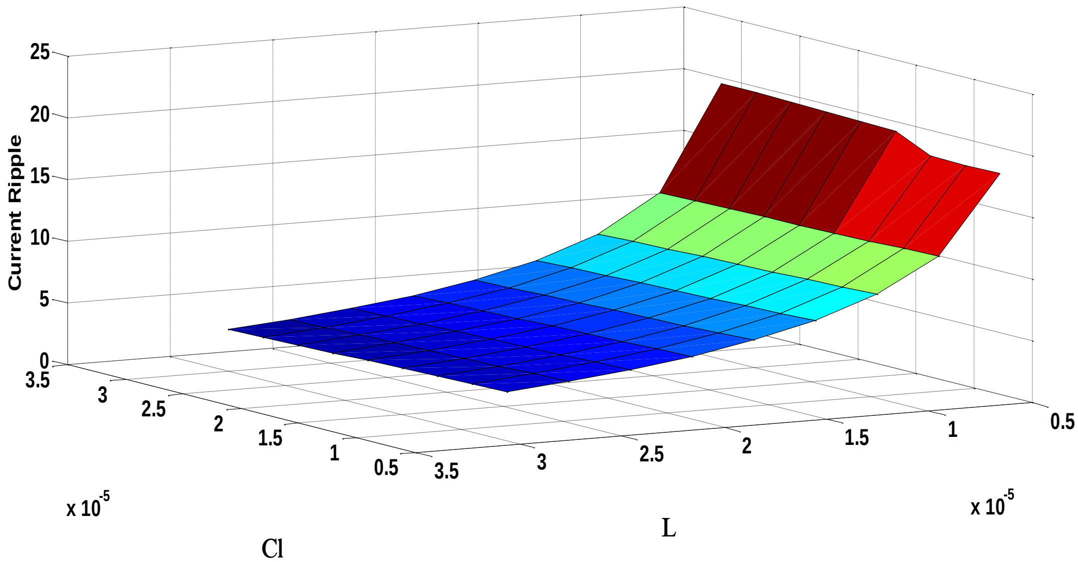

Figure 4-8 Current ripple performance

Regarding selecting C_l, the trends shown in Figures 4-7 and 4-8 indicate that the smaller C_l provides good power output with reduced ripple. In this research, the final C_l is chose as 10 μF. The parameter needed to be determined is L. Different from C_l, the power output and current ripple is a trade-off function of the inductor value L. To make a reasonable tradeoff of the power output and current ripple, the L is selected as 16μH. At this value, the circuit yields reasonable power output with low ripple at the same time.

4.4. Conclusion

In this chapter, the effects of parameters of the buck converter are studied in simulations. The three main parameters are capacitors C_t, C_l and the inductor L. The method of selecting these parameters are based upon numerical simulation results using the developed Simulink model. After studying the parameters sensitivity to the power output and current ripple, it is concluded that C_l should be small and C_t and L have a trade-off relationship with respect to power output and current ripple.

The following table lists the selected parameter for the buck converter circuit.

Table 4-4 Selected parameters

C_t	C_l	L
400 μF	**10 μF**	**16 μH**

Chapter 5 Controller Design

As the center piece of the thermoelectric generator circuit, the buck converter is going to work under different load. Controlling the buck converter to adapt to the varying load resistance for the maximum power output is the central target for controlling the duty-cycle.

5.1 Relationship between Power Output and Duty Cycle

Before designing the controller for the buck converter, we are going to study the relationship between power output and duty cycle. With this relationship, the control strategy can be developed. Figure 5-1shows the simulation results with load resistance defined in Table 5-1. Note that each simulation response is associated with a unique load resistance.

Table 5-1 Parameters of buck converter (4)

C_t (μF)	C_l (μF)	L(μH)	R_t (Ω)	Duty Cycle (%)
400	10	16	0.05:0.05:0.6	10:1:90

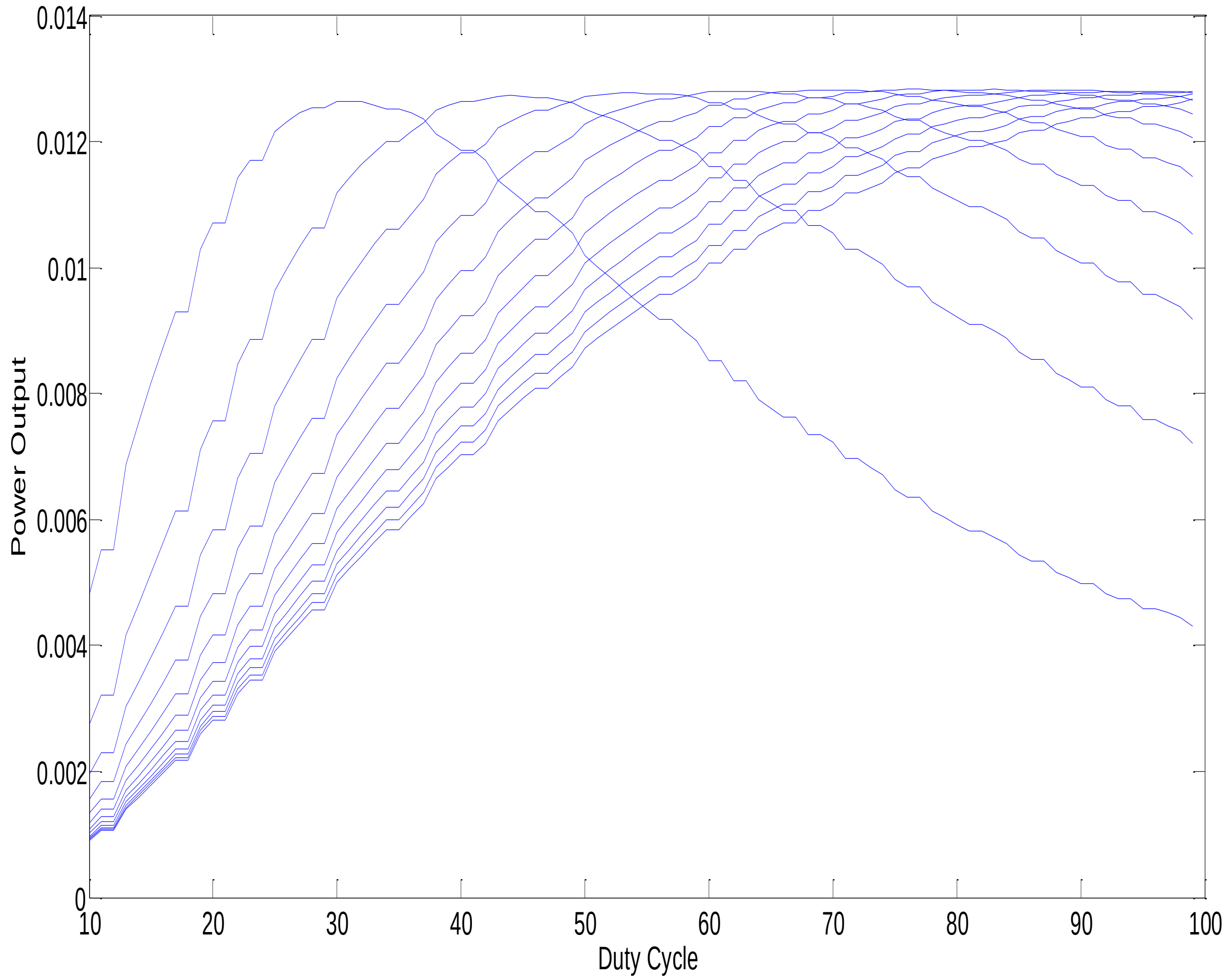

Figure 5-1 Power output performance

Twelve simulations were conducted with the load resistance varying from 0.05Ω to 0.6Ω. From Figure 5-1, it is obvious that all the response curves have only one peak point. That is the maximum power output point. The power output increases as the duty cycle goes up until it approaches maximum. After the peak, the power goes down.

For this reason, the extreme seeking control theory is used to a good fit for the buck converter duty cycle control to maximize the output power.

5.2. Extreme Seeking Control

In this section, we are going to introduce extreme seeking control theory. Extreme Seeking is used in the field that the system transfer function is unknown or very complicated. It can be used as a method to optimize steady-state performances for certain system with guarantee stability [18]. It was widely used in wind energy [19] and ABS system in vehicle [20].

In this research, the target buck converter is a periodic system with a PWM controlled switch. In this case, the controller can be designed using a deterministic extreme seeking scheme as shown in following block diagram in Figure 5-2.

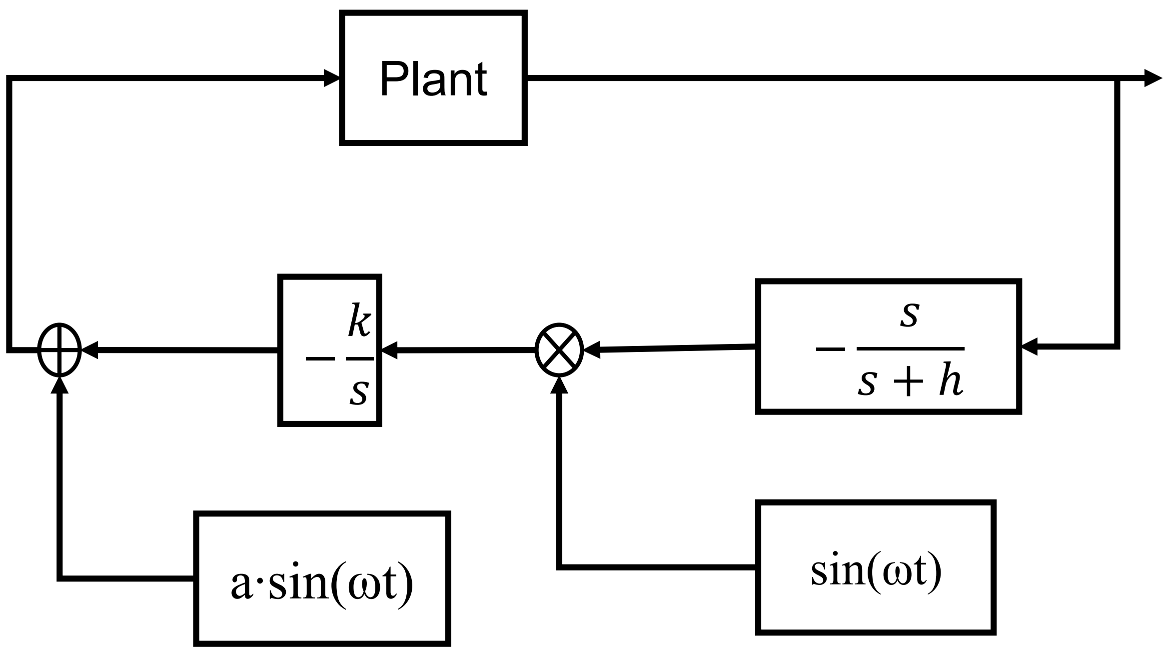

Figure 5-2 Block diagram of extreme seeking scheme

The signal sinusoid is the perturbation applied to the system. The output of the plant goes through a high-pass filter to obtain the derivative of that output. Note that the derivative provide the information of system response to the perturbation. Then, the derivative signal is multiplied with the white perturbation and the result is integrated to form the extreme seeking control signal with gain k. Thus, the extreme value, power output, is achieved when the derivative approaches zero [21].

5.3. Simulation Model with Controller

With the extreme seeking scheme shown in the last section, it is simple to build a simulation model with the extreme seeking controller as shown in Figure 5-3. In order to implement the associated duty cycle control, a new pulse input model is to make it controllable. The real-time power output signal is selected as the feedback signal. The Simscape mode is used as the plant model, shown in figure 5-4.

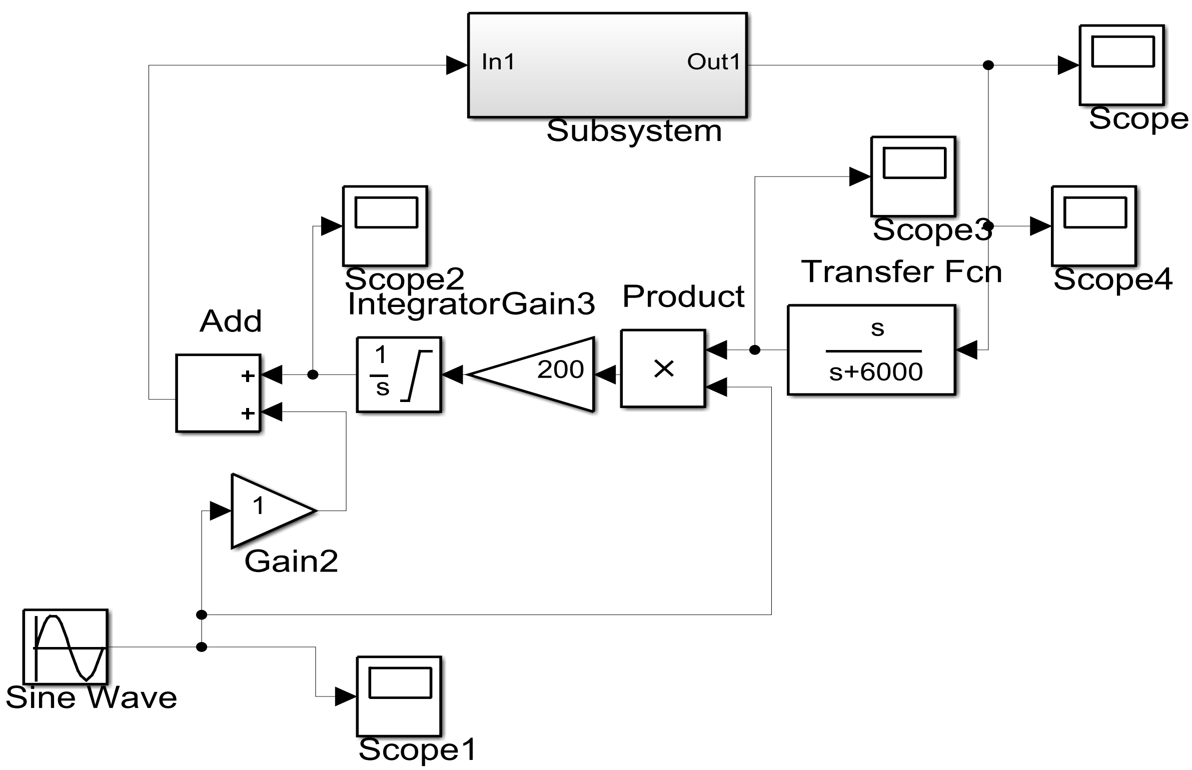

Figure 5-3 Simulation model of extreme seeking controller

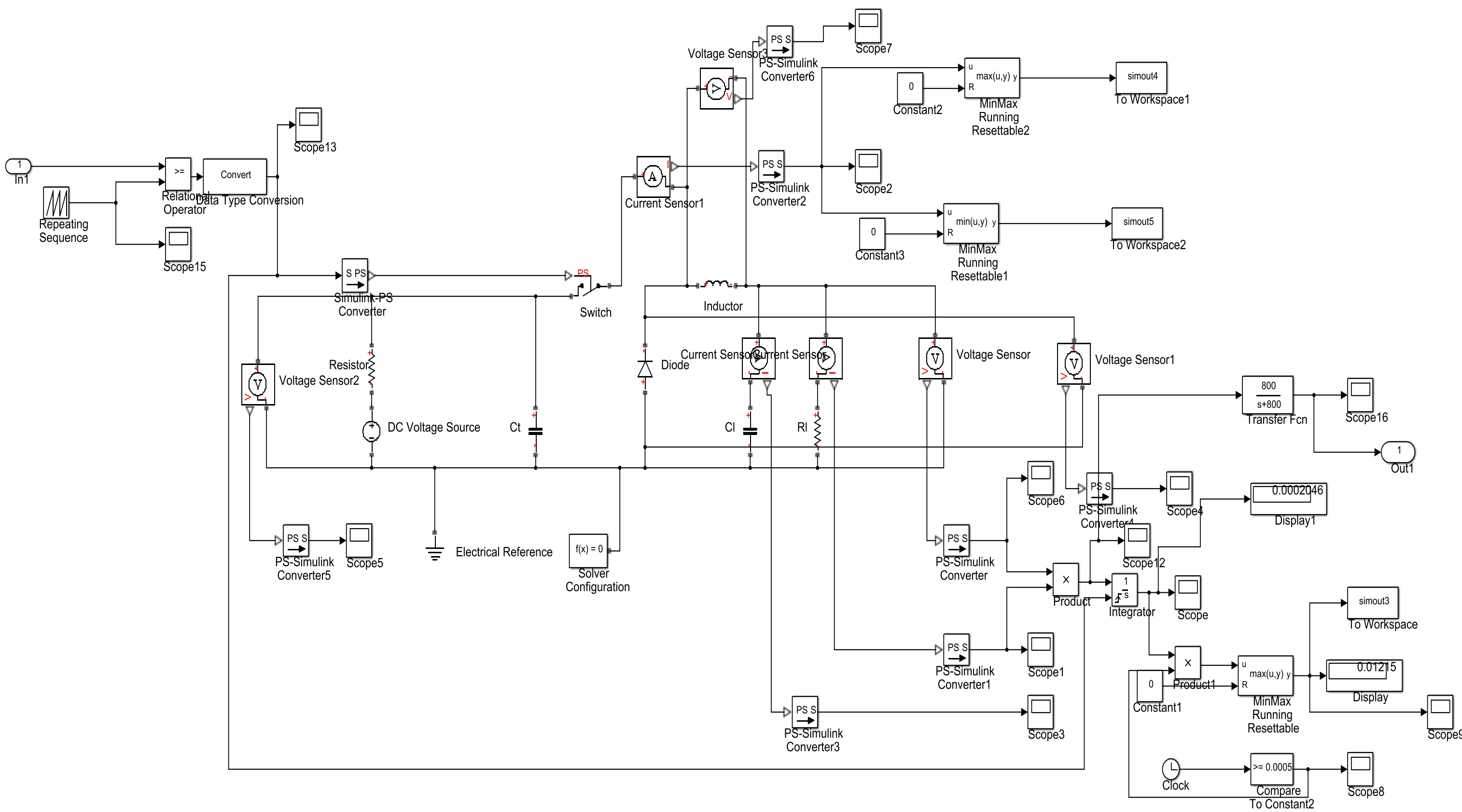

Figure 5-4 System Plant Simulation Model

5.4. Simulation Result

After building the extreme seeking controller system model, several simulations were conducted to verify the performance of the extreme seeking.

Table 5-2 Simulation parameters of controlled buck converter

C_t (μF)	C_l (μF)	L(μH)	R_t (Ω)
400	10	16	0.2

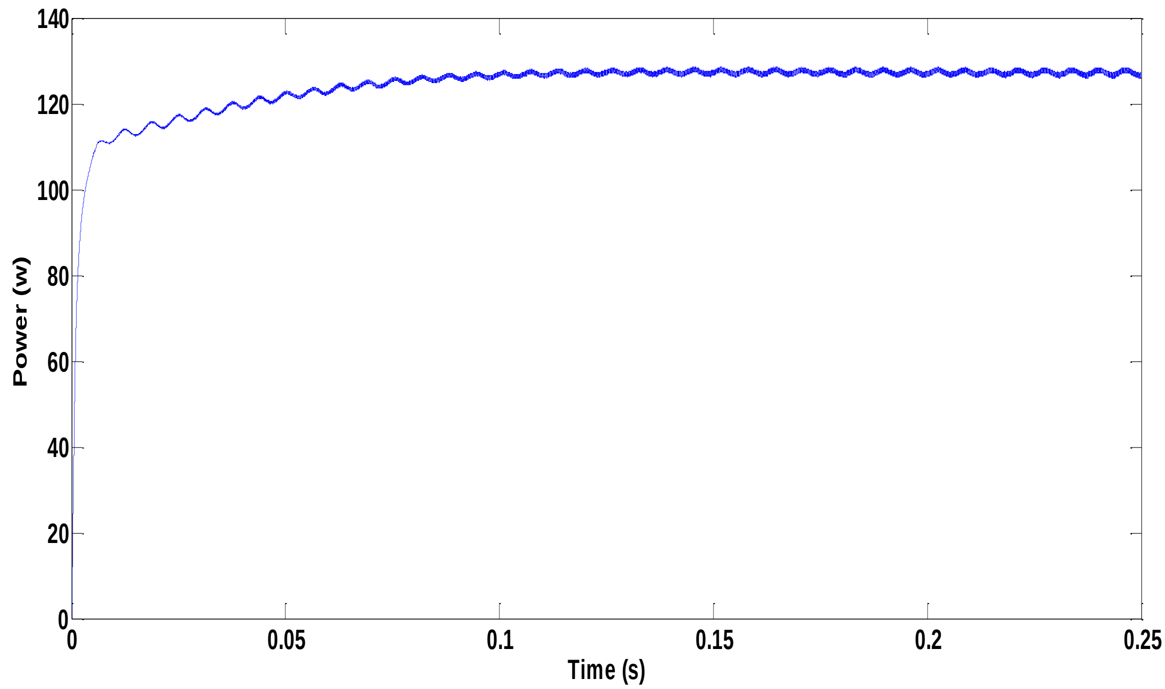

Figure 5-5 Power efficiency of the Buck Converter

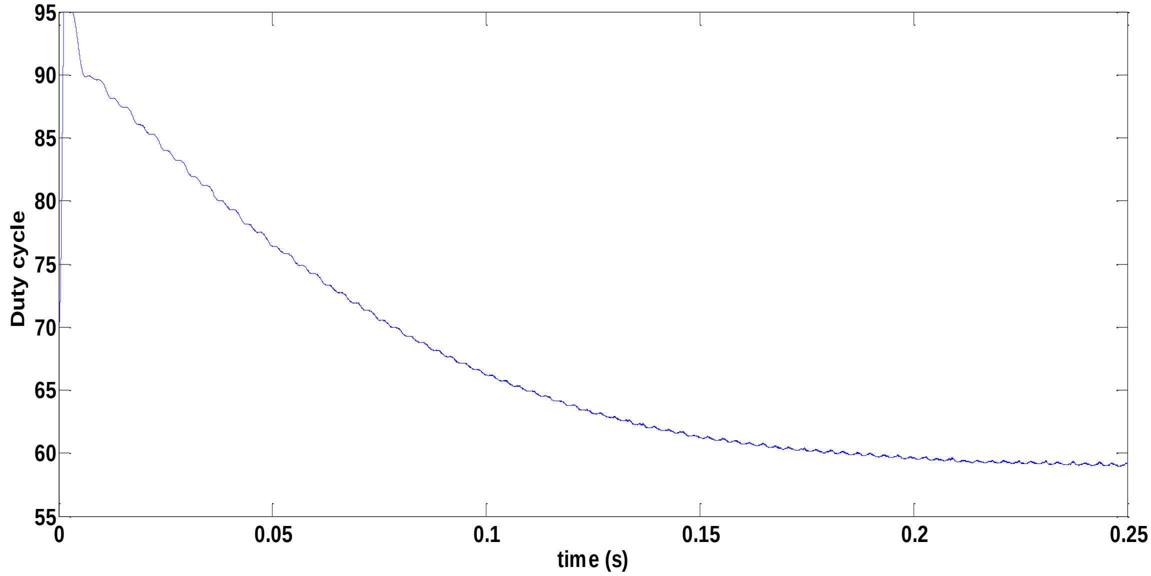

Figure 5-6 Duty Cycle of Buck Converter

In figure 5-5, the power output of the buck converter is stable at around 120 W. Compared with the circuit without control, the power is much higher.

The duty cycle curve in Figure 5-6 also shows that the extreme seeking controller converges after 0.2s, and the optimized duty cycle is stabilized at around 60. This also matches the result shown in Figure 5-1 that the best duty cycle is around 60 with the load resistance of 0.2Ω.

5.5. Conclusion

By using extreme seeking scheme, a controller is designed for the buck converter to optimize the power output in real-time and the simulation results shows that the control converges in 0.2s.

Chapter 6 Conclusion and Future Work

The load resistor of the thermoelectric generator varies as lead changes. This could lead to degrade performance of the thermoelectric generator. In order to overcome this problem. A buck converter circuit is designed, modeled, and optimized to maximize the thermoelectric generator power output. An extreme seeking controller is also designed for the buck converter to maximize the power output under different load resistant level.

6.1 Conclusion

As a switch regulation device, buck converter is proved to have high efficient and small size compared with the linear supply source. In this research the buck converter applied in thermoelectric generator, and a PMW signal was used to regulate circuit for maximal power output as the load resistance changes.

In order to optimize the buck converter, matlab Simscape tool box is used to develop simulation model of target buck converter. The Simscape model is verified the model with differential equation analytical model, the state-space simulation model. The sensitivities of different parameters, such as the capacitors and inductor in the buck converter, are obtained through intensive simulation study, and the optimal set of parameters. The main performance indexes used to evaluate parameter sets are current ripple and power output. With the help if the extreme seeking control scheme, the buck converter can be controlled in real-time with maimal power output when the load resistance changes.

6.2. Future Work

The next step is to develop a real physical buck converter for the thermoelectric generator to verify the modeling and control results presented in this thesis, the extreme seeking controller need to be verified next.

BIBLIOGRAHY

BIBLIOGRAPHY

[1] Matthew Lyle, "The Design, Development, Fabrication and Testing of a 100 Watt Skutterudite Thermoelectric Generator", Michigan State University,2011.

[2] Caltech, "A Brief history of Thermoelectric", California Institute of Technology.

[3] National Aeronautics and Space Administration, "Multi-Mission Radioisotope Thermoelectric Generator (MMRTG)", NASAfacts.

[4] S.E. Jo, M.K. Kim, M.S. Kim and Y.J. Kim, "Flexible thermoelectric generator for human body heat energy harvesting", ELECTRONICS LETTERS, 2012

[5] "BMW provides an update on waste heat recovery projects: Turbosteamer and the Thermoelectric Generator", Green Car Congress, 2011

[6] Qiang He, Yixin Zhao, "The Design of Controller of Buck Converter", International Conference on Computer Application and System Modeling, 2011

[7] Saurabh Srivastava, Yashwant Kumar, A. Misra, S.K.Thakur and V.S. Pandit, "Optimum Design of Buck Converter Controller using LQR Approach", IEEE CONFERENCE PUBLICATIONS, 2013

[8] A. Morra, M. Piselli, M. Flaibani, A. Gola, "A Buck Converter Operating in PFM mode, Mathematical Model and Simulation Analysis", IEEE CONFERENCE PUBLICATIONS, 2007

[9] Chengwu Tao, and Ayman Fayed, "Output Spectrum Analysis of Buck Converters in DCM with PFM Control", IEEE CONFERENCE PUBLICATIONS, 2012

[10] Chu-Hsiang Chia, Pui-Sun Lei, Robert Chen-Hao Chang, "A High-Efficiency PWM DC-DC Buck Converter with a Novel DCM Control under Light-Load", IEEE CONFERENCE PUBLICATIONS, 2011

[11] Mamun Rabbani, Student Member IEEE, H. M. Mesbah Maruf, Tanvir Ahmed, Md. Ashfanoor Kabir, Member IEEE, yUpal Mahbub, Member IEEE, "Fuzzy Logic Driven Adaptive PID Controller for PWM Based Buck Converter", IEEE CONFERENCE PUBLICATIONS, 2012

[12] Ghulam Abbas, Nacer Abouchi, Awais Sani, Cyril Condemine, "Design and Analysis of Fuzzy Logic Based Robust PID Controller for PWM-Based Switching Converter", IEEE CONFERENCE PUBLICATIONS, 2011

[13] ANASRAJ R. , SUSY THOMAS, “Design of Initial Conditions Based Sliding Mode Controller for Buck Converter”, IEEE CONFERENCE PUBLICATIONS, 2008

[14] Siew-Chong Tan, Y. M. Lai, Chi K. Tse, and Martin K. H. Cheung, “A Fixed-Frequency Pulsewidth Modulation Based Quasi-Sliding-Mode Controller for Buck Converters”, IEEE CONFERENCE PUBLICATIONS, 2005

[15] Yen-Wu Lo Roger J. King “Sampled-Data Modeling of the Average-Input Current-Mode-Controlled Buck Converter”, IEEE TRANSACTIONS ON POWER ELECTRONICS, 1999

[16] Fei-Hu Hsieh, Nie-Zen Yen, and Yau-Tarng Juang, “Optimal Controller of a Buck DC–DC Converter Using the Uncertain Load as Stochastic Noise”, IEEE Transactions on Circuits and Systems, 2005

[17] Xiong Du, Luowei Zhou, Heng-Ming Tai, “double-frequency buck converter”, IEEE Transactions on Circuits and Systems, 2009

[18] Alexander Scheinker, “Extreme Seeking for Stabilization”, University of California Ph.D. dissertation, 2012

[19] Azad Ghaffari, Miroslav Krsti´c, and Sridhar Seshagiri, “Power Optimization and Control in Wind Energy Conversion Systems using Extreme Seeking”, American Control Conference, 2013

[20] Chunlei Zhang, Raúl Ordóñez, “Extemum-Seeking control and Application”, Advances in Industrial Control, 2009

[21] S.-J. Liu, M. Krstic, “Stochastic Averaging and Stochastic Extremum Seeking”, Communications and Control Engineering, 2012